Order Number 9130383

Structural analysis and applications of polymer networks formed from surface-active copolymers in aqueous solvents

Varelas, Charalambos G., Ph.D.

City University of New York, 1991

U·M·I
300 N. Zeeb Rd.
Ann Arbor, MI 48106

STRUCTURAL ANALYSIS AND APPLICATIONS OF POLYMER NETWORKS FORMED FROM SURFACE-ACTIVE COPOLYMERS IN AQUEOUS SOLVENTS

By

CHARALAMBOS G. VARELAS

A dissertation submitted to the Graduate Faculty in Engineering in partial fullfillment of the requirements for the degree of Doctor of Philosophy, The City University of New York

1991

This manuscript has been read and accepted for the Graduate Faculty in Engineering in satisfaction of the dissertation requirement for the degree of Doctor of Philosophy.

May 16, 1991
Date

Prof. Carol A. Steiner
Chair of Examining Committee

5/16/91
Date

Dean Gerard Lowen
Executive Officer

Prof. Charles Maldarelli

Prof. Leslie L. Isaacs

Prof. Gabriel Tardos

Dr. Bret Berner

Supervisory Committee

THE CITY UNIVERSITY OF NEW YORK

ABSTRACT

STRUCTURAL ANALYSIS AND APPLICATIONS OF POLYMER NETWORKS FORMED FROM SURFACE-ACTIVE COPOLYMERS IN AQUEOUS SOLVENTS

by

Charalambos G. Varelas

Adviser: Professor Carol A. Steiner

The structure and properties of dispersed phase hydrogels made from surface-active graft copolymers have been investigated using fluorescence spectroscopy, rheology and calorimetry. In addition, the solute retention and release properties of these gels have been investigated with an eye toward applications in controlled drug release devices. A mathematical model was developed which we will ultimately use to predict the release behavior of our gels from their structure.

The graft copolymer used in this study is hydrophobically modified hydroxyethyl cellulose (HMHEC). It is composed of a water-soluble backbone to which hydrophobic grafts are covalently bonded. We have shown that the polymer phase-separates in water/alcohol solvents due to the inherent incompatibility of certain of the polymer segments with water. That leads to the formation of amphiphilic hydrogels that exhibit unique swelling properties in the solvents. These hydrogels are clear, flexible and

viscoelastic. They are composed of hydrophobic microdomains dispersed throughout the bulk phase, that can sequester hydrophobic solutes and release them over time. These unique properties make these hydrogels potentially advantageous in applications such as separation processes and controlled release of pharmaceutical agents.

The results presented here is be divided into 4 principal conclusions. First, the best hydrogels form at 50/50 (v/v) ethanol/water solvents and at polymer concentrations higher than 0.6% (w/w). By best gels we mean the most stable in structure with the highest storage modulus. Second the hydrogels are characterized by microdomains which are hydrophobic, not in contact with water and stable to drying and swelling. At low shear stress, the microdomains behave as temporary linkages of finite lifetimes. The molecular weight between microdomains was found to be independent of the volume fraction of polymer in the gel. The number of linkages per backbone ranges from 22.8 ± 1.3 to 26.2 ± 1.5 over the frequency range 30-50 rad/sec. Third 1% HMHEC gels can absorb tryptophan and theophylline at average levels 73 ± 3%, and 50 ± 7% higher than water and release the solutes at a constant rate for 8 and 10 h, respectively. Fourth, the mathematical model developed can be used in conjunction with our structural characterization results to predict the optimum gel composition for a particular release profile.

ACKNOWLEDGMENTS

I am indebted to numerous people who have helped me and encouraged me to start and complete this work. First and foremost I would like to acknowledge my advisor, Professor Carol A. Steiner, for her suggestions, encouragement and patience during the course of my research. It was her support, inspiration and friendship that made this work possible. I wish to thank Dr. Bret Berner from Ciba-Geigy Corp. for serving on my committee and for contributing to my research with many useful remarks and suggestions. I would like to thank Professors Charles Maldarelli, Leslie Isaacs, Gabriel Tardos and Roberto Mauri for serving on my committee. Their many interesting ideas and questions, as well as their encouragement are much appreciated. To Dr. John Denuzzio whom I had the good fortune to work with during my visits to the Ciba-Geigy Corp., I extend heartfelt thanks for the interest he showed in my research. To the Department of Chemical Engineering of The City College of New York, I am very thankful for their support.

I would very much like to thank my friends, Dr. Abdul Dualeh, Dr. Angelo Georgiou, Dr. Ramona and Prof. Dimitri Papageorgiou for their emotional and intellectual support. To my friends, Dino, John and Galatheos who provided much-needed moral support, I am very grateful.

Lastly and more profoundly, I wish to thank my family for their love, support and courage. I was very fortunate

to have their continuous encouragement from the beginning to the end of this work.

This work is dedicated in memory of my mother Eleni.

TABLE OF CONTENTS

LIST OF FIGURES

CHAPTER 6

LIST OF TABLES

CHAPTER 1

INTRODUCTION

Microphase separation in copolymer solutions is the phenomenon that occurs when one type of copolymer segment is relatively incompatible with the solvent. The result of this separation is the aggregation of the incompatible segments among themselves in order to avoid unfavorable interactions with the solvent molecules. More specifically, in aqueous solvents the nonpolar moieties of surface active polymers aggregate into hydrophobic domains or microphases, whose composition and morphology depends on the structure of the polymer and the composition of the aqueous medium. The properties of these microdomains which form in these systems may be exploited in the design of a new class of materials that will consist of nonpolar regions dispersed throughout a hydrophilic polymer matrix. These materials may be of great value in the applications discussed below.

Amphiphilic materials of this nature are well suited to a variety of applications. Their structure and properties have been the subject of many recent investigations. These properties influence the mechanical and rheological properties as well as the transport properties of the materials. The different compatibility the two phases exhibit with respect to solutes permeating the materials as

well as the molecular rearrangement they can undergo at an interface without dissolution of the polymer make these unique materials very important. They are expected to be of great value in biomedical applications such as wound dressings and controlled drug release, in chromatography, and in other separation processes. However an extensive investigation is required in order to understand the formation and the properties of the microdomains themselves.

I present an experimental study of the structure and properties of a class of surface active graft copolymers in water/alcohol solvents. The specific copolymer used in this study is hydrophobically modified hydroxyethyl cellulose (HMHEC). It is composed of a hydrophilic backbone with alkyl chains grafted to it, at a degree of substitution high enough to render the polymer insoluble in water (Fig. 1a,1b). The properties of the microdomains have been investigated extensively in an effort to understand the phase behavior of the copolymer. The objective of this study is to characterize and optimize the gels formed with respect to their microstructure, bulk properties, transport properties and other properties of interest.

The materials formed in our laboratory consist of a hydrophilic polymer network with hydrophobic microdomains dispersed throughout the bulk (Fig. 1c,1d). The two phases therefore exhibit different compatibility and retention times with respect to solutes permeating the network. These

dispersed-phase materials are expected to be of particular value in biomedical applications such as controlled drug release for the following reason. The unique cellular structure of these materials will permit encapsulation of lipophilic solutes which can then diffuse out of the bulk at a rate which is independent of overall solute concentration in the material (zero-order release kinetics). This type of release rate is desirable in controlled drug release devices because it maintains a constant level of the drug in the body over the lifetime of the device. In addition to controlled drug release, other applications for these new materials may suggest themselves as their properties become more fully understood.

The work presented here is divided in the following format. Chapter 2 contains a summary of relevant literature from which appropriate experimental techniques were chosen. Chapter 3 gives an outline of the experimental plan. It describes the materials and the experimental techniques that were used to investigate and characterize the polymer networks. Results and discussion based on these experiments are presented in chapter 4, 5 and 6. Chapter 7 presents conclusions and suggestions for future research.

FIGURE 1

Structure of HMHEC and Gels

POLYMER STRUCTURE

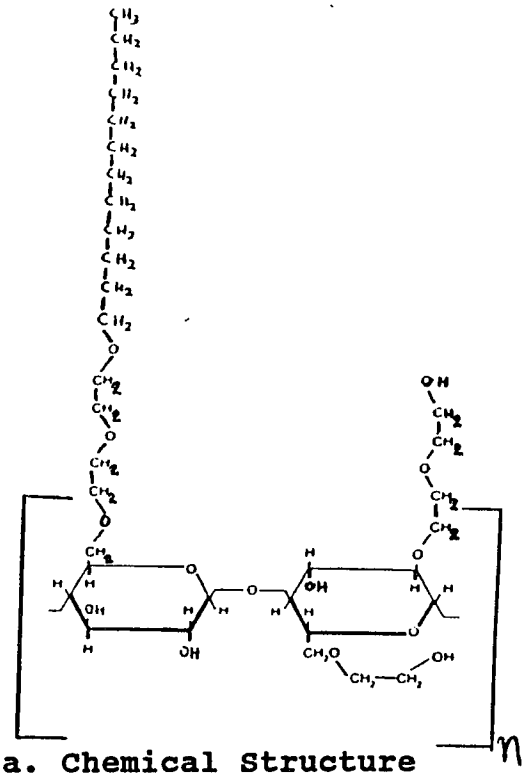

a. Chemical Structure

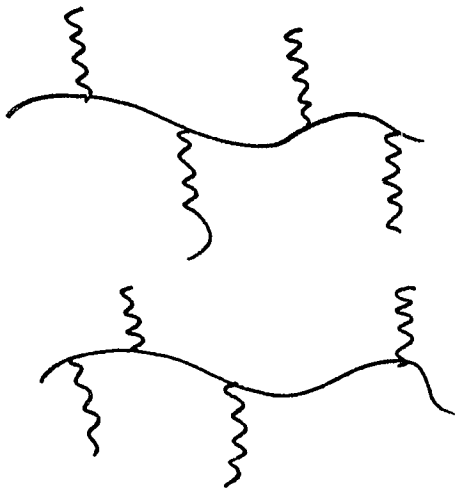

b. Physical Picture

GEL STRUCTURE

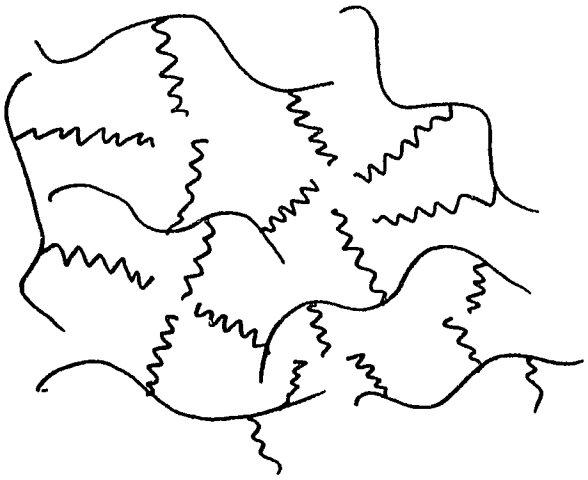

c. Physical Picture

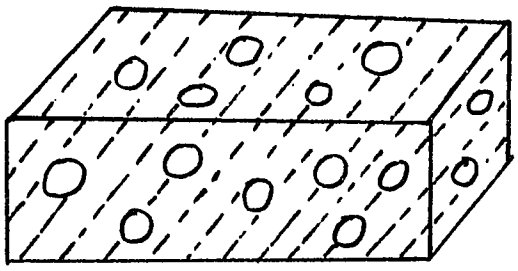

d. 3-Dimensional Picture

CHAPTER 2

LITERATURE REVIEW

The research work done so far in the field of phase separation in copolymer systems can be divided into three categories. The first deals with the phenomenon of phase separation of polymer mixtures in the presence of a solvent. The second category involves the characterization and development of polymer-solvent complexes using various experimental techniques. The third category comprises efforts to utilize the polymer networks formed by testing their biocompatibility and transport properties.

2.1 Microphase Separation of Polymer Mixtures.

Binary polymers include such important classes as block-, graft- and star-polymers. The scale of phase separation in such systems is smaller than the macromolecule's length, and such separation is therefore called microphase separation. Microphase separation of the different moieties in copolymer molecules has been documented for many materials (1-9) and is presumed to be responsible for altered bulk properties in some cases. Properties which exhibit some dependence on the structure of

the aggregates, or microdomains, include the morphological, mechanical and rheological properties, permeability, selectivity, degree of swelling of hydrogels in water and transition temperatures of the material. The microdomain composition and geometry depend in turn on the structure of the polymer and the composition, temperature, pH, etc. of the surroundings (10-15). Thus it is evident that under favorable conditions intermolecular hydrophobic interactions occur spontaneously throughout the materials, resulting in the formation of thermodynamically stable microdomains.

To date most of the work published on microphase separation in polymers has focused on block copolymers. The phase separation of block copolymers has been modeled in several cases (2,16-17) by making simplifying assumptions about the polymer structure. Various experimental techniques including X-ray photoelectron spectroscopy (XPS), differential scanning calorimetry (DSC), and viscoelastic mechanical property measurements for a variety of block copolymer architectures (AB, ABA, BAB, ABC) have been used to characterize the microphases (2,3). There is evidence that the composition of the interphase between the bulk network and the microdomains in cast films depends on the casting solvent, providing a large measure of control over the final network structure. Other authors have also established the occurrence of microphase separation in copolymer systems (4-6,20).

Krause (20) reviewed empirical evidence of the occurrence of microdomains in block copolymer membranes such as those used for reverse osmosis and ion exchange processes. Depending on whether they are dispersed or continuous, the microphases may either sequester compatible solutes or serve as channels for their transport through the membrane. Partitioning of solutes into microdomains was found to be a complex function of solute structure and microdomain structure and composition and could not easily be predicted quantitatively.

Phase separation criteria have been defined for different types of copolymers (4). From the Flory-Huggins theory (4.a) we know that a binary mixture of A and B homopolymers phase separates at a critical parameter, χ, given by:

$$(\chi N)_c = 4 \qquad (2.1)$$

when each of the homopolymers has N/2 monomer units. The quantity χ is the Flory-Huggins interaction parameter and is zero for athermal mixtures, positive for endothermic mixing, and negative for exothermic mixing. Leibler (18) found that a 50:50 diblock AB copolymer containing N monomer units has a larger critical χ value:

$$(\chi N)_c = 10.5 \qquad (2.2)$$

Since $\chi \sim 1/T$ (T is the temperature), this shows that phase separation is more difficult (requires a lower temperature)

in diblock copolymers than in homopolymer systems. We can see from the above equations that the critical temperature required for phase separation when two homopolymers of the same size are chemically combined to form a diblock copolymer reduces by a factor of 2.6.

It has been shown (4) that it is even more difficult to phase separate a graft copolymer than a corresponding diblock copolymer. This is attributed to the different entropies in the two copolymers. Although the entropies of graft and diblock copolymer melts are nearly equal, the entropies of the ordered phase-separated structures are different and the entropy change associated with the disorder-to-order transition of a graft copolymer is greater than that for the corresponding diblock. Since the heats of transition for both graft and diblock are essentially equal, the larger entropy change for the graft copolymer requires a larger $(\chi N)_c$ for the graft copolymer. Thus, relatively little work has been reported on microphase separation in graft copolymers.

Graft copolymers represent an important class of network-forming surface-active polymers because they can be produced easily from synthetic and naturally-occurring homopolymers such as poly(vinyl alcohol), cellulose derivatives, etc. (19). The physical characterization of graft copolymers composed of alkyl side chains on a water soluble backbone has been the subject of much work (21,22)

and it has been shown that in the presence of certain solvents the grafts aggregate into microdomains composed primarily of the hydrophobic chains. This goes against recent theoretical predictions (4) that these polymers should not be driven to microphase separate at any total concentration of side chains. Thus, in the presence of some solvents the behavior of the polymer changes and results in phase separation of the grafts.

The solution properties of block and graft copolymers as well as structural information about the microdomains, specifically the size and the geometry of the polymer bound aggregates, have been obtained using fluorescence spectroscopy (25,26,29), small angle neutron scattering (30-36,38) and rheology (45-49).

2.2 Controlled Release From Polymeric Materials.

Controlled drug release is an emerging technology arising from a need to prolong and improve delayed drug administration. With conventional drug delivery systems (e.g. pills, injections) the drug concentration in the blood rapidly reaches a maximum and then falls to a low level, so that repeated drug delivery is needed to maintain an effective level of drug in the body. The pattern of drug release may thus be constant, oscillating, declining continuously, or even pulsating periodically. Such drug delivery systems may result in alternating periods of

toxicity and inefficacy. On the other hand, controlled release systems would maintain a desirable drug concentration between toxic and ineffective levels. The pattern of release would be a qualitative design feature of the system. A number of water swellable networks or hydrogels have been tested and used for controlled drug release (51-53).

2.2.1 Different types of drug delivery systems

There are several types of drug delivery systems available to therapists today. The materials selected for incorporation into any of these systems must not only provide the intended mode of operation but also be biocompatible and compatible with the many constraints imposed by manufacturing. For example, diffusional drug delivery systems must utilize membranes whose permeability is highly reproducible and stable in the presence of biologic fluids. The long-term biologic exposure will lead to absorption of a variety of low-molecular-weight components that have the potential for altering polymer permeability or interacting with the drug in the reservoir so as to inhibit its subsequent release. Thus, there are different considerations that one must utilize in selecting a material for use in a controlled drug delivery system. Some of the types of release systems existing today include: buccal, ocular, uterine, bioerodible, transdermal and

infusion drug delivery systems. All of them are attached to or inserted in soft tissue of the body. For example, a buccal drug delivery systems consisting of an adhesive polymer layer, a reservoir polymeric layer and an impermeable backing, is attached to the mucosa. This kind of system needs to be removed after therapy. Thus, the adhesiveness must be sufficient to prevent detachment but on the other hand should not be so strong as to damage the mucosa upon removal. A transdermal system works the same as way as a buccal one, and it may be attached to the skin surface. Ocular drug delivery systems which are used for treatment of ophthalmic disorders, reside in the cul-de-sac of the eye. These systems must be adequately flexible and soft so they can adjust when they are inserted in people's eyes with different cul-de-sac dimensions. Similarly, infusion drug delivery systems which are used for critically ill patients who need continuous therapy must meet special requirements. They must be compatible with the active agent so that there are no undesirable reactions or physical interactions. They must be mechanically stable to avoid rupture of the reservoir and excessive release of drug and flexible to avoid local tissue damage during drug refilling. Hydrogels are suitable candidates for these delivery systems because of their high flexibility and biocompatibility. In addition, hydrogels have been used in the development of new artificial coverings, which will meet the requirements faced

in the treatment of major skin wounds. The work has been focused on finding polymeric membranes that would be impermeable to microbes from the environment, capable of adhering well to the wound, and be easily removable without causing any damage to the tissue beneath the cover. Moreover the membranes should have optimal water permeability to prevent either desiccation of the wound or fluid accumulation under the covering.

Our hydrogels have potential in the development of the above systems, because they meet many of the special requirements. They are not toxic which eliminates the risk of unfavorable interactions with the active agents. Moreover, their viscoelastic behavior provides adequate flexibility and mechanical strength .

2.2.2 **Controlled release systems from polymeric materials**

The first controlled drug delivery system was reported by Folkman and Long (54) in the mid-60s. They indicated that one could encapsulate lidocaine, a cardioregulatory drug, within a tube of silicone rubber and implant it in the myocardium of an experimental animal, and the drug would be released over a prolonged period of time providing some measure of control of myocardial rhythm. The drug was released by the mechanism of dissolution in the silicon rubber and then it diffused through the rubber into the myocardium. Soon other drug delivery systems were developed

based on the same principles (55,56).

Since then, extensive analysis of a variety of controlled release systems has been done. Langer and Peppas (57-59) and Peppas and Gurny (60) have reviewed various aspects of the preparation, structure and biocompatibility of polymers for pharmaceutical applications. Based on the type of mechanism that controls the release of drug incorporated in a polymeric system, Langer and Peppas (58) have divided the release systems into four categories: diffusion-controlled, chemically-controlled, solvent-activated, and magnetically-controlled devices. Of these four the diffusion-controlled and the solvent-activated devices have received the most attention. This is because in most applications the desired drug release behavior is zero order, that is, the drug delivery rate is independent of time over long periods. It has been shown that systems that can exhibit zero-order kinetic behavior in vitro include reservoir and matrix diffusion-controlled devices (57-60), as well as solvent activated systems (swelling-controlled) when the macromolecular relaxations of the polymer controls the diffusional release of the drug (61). In matrix-type systems the drug is dispersed or dissolved in a polymer solution, the solution is evaporated, and a homogeneous slab, sphere, disk or cylinder is prepared (62). These types of systems have been designed based on mathematical predictions of the release behavior in vitro, using the

solutions of the Fickian equation (63,64). In solvent-activated release systems the bioactive agent is dispersed into the polymer to form non-porous films.

An example of controlled release from a matrix-type device is given by studies of the release rates of 1,3-bis(2-chloroethyl)-1-nitrosourea (BCNU) from various kinds of silicone and silicon-nylon devices (67). BCNU was injected into the devices and then they were placed into distilled water. By measuring the concentration of BCNU in the water over time, it was shown that steady state was reached. The release rate was predicted using the fact that the rate is controlled by the membrane permeability to the drug and the configuration of the device (i.e., surface area, and wall thickness) (68,69). The mass transfer of drug from the device observed Fick's law in the form:

$$\frac{dM_t}{dt} = \frac{A \Delta K \Delta C}{L} \qquad (2.3)$$

where M_t is the mass of drug released, dM_t/dt is the steady-state release rate, A is the surface area of the device, ΔK is the drug permeability coefficient of the membrane, ΔC is the difference between the internal and external drug concentrations, and L is the wall thickness (68). It was assumed that the external concentration of BCNU is much lower than its internal concentration, giving a constant concentration difference. In practice this requires a high loading of drug in the device. Thus, the release rate of

drug from diffusion-controlled matrix-type devices is predicted to be related linearly to the surface area of the device and reciprocally to the wall thickness.

Release behavior can also be analyzed using the equations that describe the fraction of the drug released, M_i/M_∞ and the rate of drug released per surface area, dM_i/Adt:

$$\frac{M_i}{M_\infty} = kt^n \tag{2.4}$$

and

$$\frac{dM_i}{Adt} = nc_d k t^{n-1} \tag{2.5}$$

where M_i is the amount of drug released at time t, M_∞ is the amount released at infinite time which actually represents the total amount of drug incorporated in the device initially, and c_d is the initial concentration of drug in the polymer. The constants k and n are parameters that depend on the specific polymer/drug solvent system. Peppas (65) has discussed possible values for the exponent n.

Although several mathematical models have been developed to describe the diffusion of drugs across polymeric membranes, a study on the release of a solute embedded in a dispersed phase material has not been presented. Therefore, in the present study we have develop a mathematical model that predicts the release of hydrophobic solutes from our dispersed-phase materials. The

model is based on the same concepts set by other investigators (63-69) such as Fick's law of diffusion. The additional work needed in our case is to account for the release of the solutes from the dispersed phase into the bulk phase.

2.2.3 Controlled release systems from amphiphilic polymers.

During the last decade, increasing attention has been paid to controlled drug delivery systems made from amphiphilic polymers. Because of their unique structure, potential applications of amphiphilic materials may be quite extensive. We have seen a dramatic increase in research studies involving applications, especially pharmaceutical, of amphiphilic materials. Most of these studies involved the preparation, structural analysis and biocompatibility of polymeric devices used as drug delivery systems (50-64). A great variety of responses must be avoided to meet the requirement of biocompatibility, i.e., immunologic reaction, thrombus formation, alteration of plasma proteins, denaturation of enzymes, tissue destruction or damage, carcinogenesis, and adverse effects due to toxic contaminants or by-products in the material.

Amphiphilic materials are better candidates than other polymeric materials for release systems because they are

more flexible and less toxic (70). The release kinetics of drugs in various amphiphilic systems has been studied extensively. Amphiphilic networks made of copolymers of methacryloyl-capped polyisobutylene (MA-PIB-MA) with 2-(dimethylamino)-ethyl methacrylate (DMAEMA) have been examined by Chen and Kennedy (66). Bromophenol blue and folic acid were used as model compounds for drug release. Diffusion of these drugs from loaded networks showed a marked pH dependence. Under specific well-defined conditions (MA-PIB-MA/DMAEMA content, PH, time range) they showed that the release of the drug was independent of time (zero order release). They also showed that the best biocompatibility of the materials was exhibited when there was a balance of the hydrophobic and the hydrophilic properties. This was found by testing the hemocompatibility of hydrogels with varying hydrophilic/hydrophobic contents and comparing bacterial types present in the blood and the implant tissue. It was suggested that interactions of biomaterials with bacteria and tissue cells are directed not only by specific receptors and surface molecules but also by the atomic geometry and electronic state of the biomaterial surface. It was found that hydrophobic materials exhibited bacterial adhesion and poor tissue compatibility, but enhanced albumin adsorption and prolonged clotting times, relative to unmodified hydrophilic materials (76). Thus, amphiphilic materials with high hydrophilic or hydrophobic

contents exhibited poor biocompatibility, while those of intermediate composition showed much better biocompatibility.

In conclusion, major advances have been made regarding the development of polymeric systems for use in drug delivery. In spite of these accomplishments the technology is limited by a lack of adequate biomaterials.

The experimental plan presented was designed to develop and characterize polymeric materials with potential applications in drug delivery. This new class of polymeric hydrogels, namely hydrophilic gels with hydrophobic microdomains dispersed throughout, is expected to be of particular value as a medium for controlled drug release. The two phases present exhibit different compatibilities and retention times with respect to solutes permeating the network. Thus the microdomains will act as reservoirs for lipophilic drugs. The drug diffuses from the reservoirs to the bulk (aqueous) phase of the gel, and from the bulk to the delivery site. Zero-order release kinetics is expected since the concentration of drug in the bulk phase will be kept constant at the saturation level of the drug. This is ensured by the high overall interfacial area between the reservoirs and the bulk compared with the interfacial area between the device and the delivery site. Thus the bulk phase will be continually and rapidly replenished with drug.

Another advantage of our hydrogels is their anticipated biocompatibility. The surface-active polymers from which the gels are made can rearrange at an interface without damaging the integrity of the gels. A dynamic interface has been shown (72-74) to be an important factor in biocompatibility of materials. However, molecular rearrangement can lead to instability of the bulk of many materials, resulting in dissolution of the polymer (73). The new materials discussed here are stable to molecular rearrangement at the surface because of the high degree of association (i.e. pseudo-crosslinking) by hydrophobes throughout the bulk. A heterophase surface is characteristic of normal vascular endothelial tissue (74) and is considered to be an important factor in the blood compatibility of synthetic materials as well. Low platelet adhesion and enhanced albumin adsorption have been reported for both block (74) and graft (75) copolymer materials with microphase-separated surface structures. The polymer molecules at the surface of these materials are able to rearrange in order to minimize the interfacial free energy when environmental conditions change (73).

CHAPTER 3

EXPERIMENTAL SECTION

3.1 Materials and Methods

The polymer used for this work is a water-insoluble hydrophobically modified hydroxyethyl cellulose (HMHEC). HMHEC is a graft copolymer whose backbone, hydroxyethyl cellulose (HEC), is a water-soluble cellulose derivative. Alkyl groups are grafted at random sites along the backbone, rendering the polymer insoluble in water. This polymer is patented by Aqualon Co., Wilmington, Del. and is available with a range of molecular weights, hydrophobe chain lengths, and hydrophobe concentrations. In our study, HMHEC, MW~10^6, with a molar substitution (MS) of 3.8 ethylene oxide (EO) groups per anhydroglucose unit and a hydrophobe degree of substitution of 1.33% (w/w) alkyl grafts (corresponding to ~78 side chains per backbone) was used. HEC with the same molecular weight and molar substitution of 2.5 ethylene oxide groups per ring was used in the experiments as the control material, permitting us to identify those effects which are due exclusively to the presence of the side chains. Ethanol/water at various compositions was used as the solvent. Solutions were prepared by stirring overnight at room temperature (~25°C). Solutions were covered during stirring to prevent evaporation of the solvent. Gels

formed 2-3 days after stirring was stopped. The experimental techniques used to characterize the hydrogels, included viscometry, surface tension, DSC, fluorescence spectroscopy and rheology. The importance and the utilization of each of these is explained in the next sections.

For the release experiments two model compounds were used: tryptophan (Aldrich, 99%, F.W. 204.23) and theophylline (Aldrich, 99%, F.W. 180.17), with structural formulas :

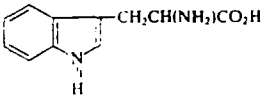

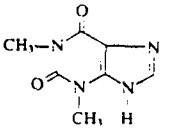

Tryptophan **Theophylline**

Their solubilities in water at 25°C, are 11.4 g/L and 7.0 g/L respectively. Both compounds were used as received by the manufacturer. The concentrations of the solutions were analyzed spectroscopically using a Lambda 2 UV/VIS Spectrometer.

3.2 Viscometry, Surface Tension and Differential Scanning Calorimetry (DSC)

Viscosities of the solutions were measured using a Brookfield cone-and-plate viscometer with a constant

temperature (25 ± 0.1 °C) circulating water bath. Surface tensions of the solutions were measured using a Wilhelmy plate-type surface tensiometer. Results allowed us to deduce the regions at which polymer segments start to aggregate. Differential scanning calorimetry (DSC) studies were conducted using a Dupont Instruments TA2100 Thermal Analyzer and 910 DSC.

3.3 Fluorescence Spectroscopy

Fluorescence is the emission of radiation by an excited atom or molecule. The emission intensity and the time scale of emission for a particular fluorophore is affected by its interactions during its excited state period (23). The different properties of the fluorophore in various environments make fluorescence spectroscopy a suitable experimental technique for determining properties of macromolecules in solution (24).

We have used fluorescence spectroscopy to detect the presence of hydrophobic regions in our systems. Fluorescence spectra of solutions were obtained using a Spex Fluorog-2 Model 112A Fluorescence Spectrophotometer, (Spex Industries, Inc., Edison NJ). The probe used was pyrene, which is a condensed aromatic hydrocarbon. Studies using pyrene as a fluorescence probe have received special consideration (24-29). Pyrene is a strongly hydrophobic

probe with low solubility in water (3×10^{-7} M). It has been shown that the vibrational fine structure intensities of pyrene at low concentrations (<1 $\times 10^{-6}$ M) in solutions undergo significant perturbations on going from nonpolar to polar solvents.

The spectrum of pyrene, (excitation wavelength, λ=310 nm) is characterized by five distinct peaks (emission wavelength: 350-450 nm). The ratio of the fluorescence intensity of the highest energy vibrational band (I_1, λ=370 nm) to the fluorescence intensity of the third highest energy vibrational band (I_3, λ=382 nm) has been shown to correlate with solvent polarity for a range of solvent structures (24). This unique dependence of the fluorescence vibrational fine structure was utilized in our investigation to determine the existence of hydrophobic regions in our systems.

Our first task was to obtain fluorescence spectra of pyrene in ethanol/water solutions as a function of solvent composition, which were used as calibration. Next spectra of pyrene were be obtained as a function of polymer concentration in both macroscopic phases of our systems, the gel phase and the supernatant phase. Also, spectra of solutions containing HEC, which is the control polymer, and Brij 30 surfactant ($C_{12}H_{25}(OCH_2CH_2)_4OH$) were obtained to compare with the spectra of solutions containing HMHEC. This allowed us to determine if the formation of hydrophobic

regions is a result of the different structure of the two polymers.

3.3 Rheometry

Rheometry is the measurement of rheological properties, that is the dependence of stress on strain and the time derivatives of strain. Most interest is attached to the behavior of viscoelastic materials (materials whose behavior is intermediate between that of an ideal elastic solid and that of a purely viscous liquid). The viscoelastic response of polymer solutions is a direct result of dynamical processes at a molecular level. These processes govern the rate of rearrangement of chain orientation and conformation. When any of the dynamic functions is plotted against frequency the graphs reveal a pattern of certain regions where the viscoelastic functions have characteristic shapes. The behavior of most cross-linked systems is characterized by three regions: the glassy, the plateau and the terminal region. These regions vary significantly with different kinds of molecular responses and their shape is a function of the molecular weight, degree and type of intermolecular association, crystallinity and glass transition temperature of the polymer.

The dynamic functions measured in a typical oscillatory

shear experiment are the complex viscosity η^*, and the complex modulus G^*. A common mode used in conducting rheological experiments is the cone and plate. This test mode is commonly used because for small gap angles, the shear rate is constant throughout the specimen. A brief description of how the cone and plate operates is as follows: The material being tested is sheared between two members normally concentric. The cone is driven to oscillate sinusoidally while the plate is fixed. This produces a steady shearing flow in the sample. The stress developed within the sample by the oscillating strain is also sinusoidal and it is in-phase with the strain for a purely elastic material. However, for a viscous material the rate of strain leads the stress by 90 degrees (out-of-phase). Thus, in describing the response of a viscoelastic material both the elastic and the viscous component are considered. The response is described by a complex modulus G^*, which is the vector sum of the storage modulus G', and the loss modulus G" and is defined as follows:

$$G^*(\omega) = G'(\omega) + iG''(\omega) \tag{3.1}$$

where the modulus $G'(\omega)$ is defined as the stress in phase with the strain in a sinusoidal shear deformation divided by the strain γ_0, $G''(\omega)$ is the stress 90 degrees out of phase with the input strain divided by γ_0, and ω is the frequency in radians/sec. The shear stress is determined from the

torque acting on the fixed member, and the calculation of shear rate requires only a knowledge of the speed of rotation and gap angle. The complex modulus is determined by the following equation:

$$G^*(\omega) = \frac{12Ta}{\pi d^3 \phi} \qquad (3.2)$$

where T is the measured torque, a is the cone angle, d is the plate diameter and ϕ is the angular amplitude.

In our hydrogels there are intermolecular interactions due to the presence of hydrophobic side chains; these interactions behave like pseudo-crosslinks under low applied shear, causing the network to respond as a viscoelastic material. Thus, we have adapted the theory of viscoelasticity for our unchemically crosslinked gels. We have conducted rheological experiments to measure the storage and loss moduli and the viscosity of our gels as a function of the shear rate. These properties can provide us with important information about the molecular structure of our polymer networks (40-45). Measurement of G'(ω) and G"(ω) permitted us to observe the dynamic behavior of the polymer network. In a cross-linked network the plateau modulus is independent of chain length and insensitive to temperature and is given by the nearly constant value of G'(ω) at intermediate frequencies (43). In our systems we did not see a real plateau, but only a shallow rise in the

storage and loss moduli. We have seen that the hydrophobic linkages behave differently at low and high frequencies. With the equation for modulus from the theory of rubber elasticity, we have used the values determined from the rheological experiments to find an apparent molecular weight for our networks $M_l(\omega)$, which is the molecular weight between linkages. The relationship can be expressed as :

$$M_1 = \frac{\rho \phi RT}{G_1} \qquad (3.3)$$

where ρ is the density of the undiluted polymer, ϕ is the volume fraction of the polymer in solution, R is the universal gas constant, and T is the temperature of the sample (44). $G_l(\omega)$ is the value of the storage modulus in the pseudo-plateau region.

Rheological experiments were conducted at the facilities of the Ciba-Geigy Corp. which were made available to us for our study. The instrument used is a 3250 Rotary Rheometer manufactured by Instron Corporation. The phase angle was measured with a Solartron frequency response analyzer to obtain the storage and loss moduli of the gels. From the rheological experiments valuable information has been obtained for our polymer networks. Results are presented in chapter 5, as part of a paper which is currently in review.

3.5 Transport properties of the hydrogels

Hydrogels are polymer networks that will absorb and swell with a significant proportion of water without dissolution. Potential applications of water-swellable networks in biological systems may be quite extensive. One example is controlled drug release. The release kinetics of solutes from polymeric devices are controlled by the physical and chemical properties of both the solute and the polymer. The properties influencing release include molecular structure of both polymer and solute and solubility of the solute within the device. In our preliminary solute release experiments we have tested the release of two compounds, tryptophan and theophylline, over time from our hydrogels. Since the size of the microdomains is not yet known to us, and thus the limiting size of solutes able to be incorporated in them has not been specified, we had to use low-molecular weight solutes. Tryptophan and theophylline appeared to be good choices for our preliminary experiments because of their size (M.W 204.23 and 180.17 respectively) and relatively low solubility in water.

Hydrogels were made from 1.0% wt. HMHEC solutions in 50/50 v/v ethanol/water using the methods described above and were left to dry in air. The solute loading process was

as follows. A dry gel disk was weighted and then immersed in 100 ml of a saturated aqueous solution of either tryptophan (solubility 11.4 g/L) or theophylline (solubility 7.0 g/L) at 25°C. After the gel had swelled to a constant volume, absorbing solute along with the water, it was removed and left briefly in air so that the solution on the surface could evaporate. The concentration of solute in the remaining solution was measured to investigate the partitioning of the solute. Then the solute-loaded gel was immersed in a beaker with 100 ml distilled water. Nearly all the gel surface area was exposed to the immersing solutions since there was no contact with the walls of the beaker but only slight contact with the bottom. The exposed surface area was different for every gel, because their swollen volume was different. The release behavior was investigated using one of two methods: a) by measuring the cumulative concentration of solute in solution over time; b) by measuring the concentration of the solute in solution at hourly time intervals and then replacing the solution with an equal amount (100 ml) of fresh distilled water. In both cases the solutions were stirred before samples were taken for measurements. It is important to note that we did not observe a change in the gel volume upon immersion in fresh water. This shows that most of the absorbed solute is sequestered away from the aqueous phase and the effect of the osmosis is not significant. The experiments were

performed at 25°C and 40°C to investigate the effect of temperature on the release. Calibration curves were obtained for tryptophan and theophylline by measuring the absorbance of solutions of known concentrations on a Lambda 2 UV/VIS spectrometer and are shown in Figure 1 in chapter 6. From these curves we were able to analyze unknown solutions and find their concentrations. A scan analysis showed that the peak maximum of the spectrum of tryptophan occurs at 278.5 nm and of theophylline at 271.1 nm. We used these wavelengths for our analysis since the baseline was flat on both sides of the peak and not offset. The concentrations were directly measured by the instrument based on the Beer-Lambert law, which gives a linear relation between the absorbance and concentration of the sample.

Chapter 4

SOLUTION PROPERTIES OF HMHEC/ETHANOL/WATER SYSTEMS

In this chapter, I present the results of viscometry, DSC, and surface tension experiments of HMHEC/Ethanol/Water systems. From these results we were able to identify the optimum solvent composition, the regions at which hydrogels are formed and their swelling properties. More discussion on the surface tension experiments is presented in chapter 7 as part of the future work.

4.1 Identification of Optimum Solvent Composition

In order to produce copolymer networks such as those described above, it is necessary first to solubilize the polymer in an appropriate solvent. By definition this means that all of the groups on the copolymer must be compatible with the solvent. Then the solution composition must be adjusted so as to drive the hydrophobic moieties into clusters, or microdomains.

Ethanol disrupts aqueous phase hydrophobic interactions by breaking the structure of the water, allowing non-hydrogen bonding species to become solubilized. Thus ethanol/water solutions are appropriate solvents for HMHEC.

The solubility of the polymer and the resulting solution and gel properties will depend on the composition of the EtOH/water solvent. We define the optimum solvent composition as the composition in which the side chains are maximally exposed to the solvent, and hence to each other, thus allowing them to associate. This corresponds to the solvent composition in which the polymer exhibits the lowest tendency to adsorb at the solution interface. According to the method of Robert and Thomas (77), the poorer the solvent the greater will be the tendency of the polymer to move to the air-solvent interface. Therefore the absolute value of the difference between the surface tension of a polymer

solution (γ) and that of the solvent (γ_0) should be a minimum where the polymer is in the "best" solvent.

Figure 4.1 shows the absolute value of the incremental surface tension ($\gamma-\gamma_0$) of 0.2% (w/w) polymer solutions as a function of solvent composition for both HEC and HMHEC over the entire composition range in which each polymer was soluble. Also shown is the surface tension of the solvent itself. The incremental surface tension of the control polymer increases with the percentage of ethanol in the solvent. This is expected since the HEC is highly water-soluble. More interesting, however, is the result from the HMHEC solution. A minimum is found in the incremental surface tension at 50% (v/v) (44% w/w) ethanol, identifying this composition as the "best" EtOH/water solvent for this polymer at room temperature. Note that this optimum solvent composition does not depend on the total polymer content of the solution, since the solution has been optimized with respect to polymer/solvent interactions. Hence 50% (v/v) ethanol/water was used as the solvent for all HMHEC solutions.

An important question was raised in the interpretation of the surface tension results. Roberts and Thomas assume that the two-component solvent is uniform throughout the system, and the surface tension differences depend only on the type of polymer-solvent system used. However in a

ternary system one of the solvents could be sequestered by the polymer molecules and result in a drop or increase in the surface tension. In our case pure ethanol has significantly lower surface tension than pure water (Fig.1) and a possible removal of ethanol from the surface would result in a rise in the surface tension of the solution. Thus, it is possible that ethanol is sequestered in hydrophobic clusters with the polymer and the composition of the solvent in the bulk phase changes. To clear up this uncertainty we have initiated dialysis experiments but since we were not able to complete this work, we have opted to draw conclusions from our surface tension results using the Roberts and Thomas method. The experiments involve dialysis of highly concentrated polymer solutions (>0.6% wt HMHEC) against ethanol/water solvents. The composition of the bath solution which initially is high in ethanol, 60-80% (v/v) may be analyzed using pendant drop tensiometry. This method is very accurate. It utilizes the video image of a pendant drop and the digitation of the image to determine the interfacial loci. Then it compares these loci with theoretical interfacial images obtained by the Young-Laplace equation, and determines the surface tension (74). Thus, if there is a tendency for ethanol to leave the bulk solution and become sequestered in clusters, the surface tension of the immersing solvent will go up.

4.2 HMHEC Networks from 50/50 Ethanol/Water Solutions

Four regions of behavior were identified over the range 0.1-1.4% (w/w) polymer in HMHEC/EtOH/water solutions. Below 0.3% (w/w) polymer, a one-phase solution formed which exhibited Newtonian behavior in steady shear rate range $11.5 < \omega < 230$ sec^{-1}. Between 0.3% and 0.6% HMHEC, the solutions are one-phase and non-Newtonian. Typical viscosity profiles of HMHEC solutions in 50% (v/v) EtOH/water are shown in Figure 4.2. These profiles remain unchanged over a period of at least 4 days as shown in Fig. 4.3, indicating that the intermolecular interactions giving rise to the non-Newtonian behavior are stable as well. Also at 0.3% polymer we observe a step increase in the surface tension of both HEC and HMHEC solutions (Fig. 4.4). This reflects an increased tendency for the polymer to remain in the bulk phase, since polymer adsorbed at the surface decreases the surface tension of the solution. This transition point is significant because it coincides with the observed transition to non-Newtonian behavior in HMHEC. Thus after the surface becomes saturated with free polymer, any additional polymer introduced into the system becomes incorporated into intermolecular aggregates, by analogy with the well-known process of micellization in surfactant/water solutions.

The polymer solutions become saturated at 0.6% HMHEC,

and at 0.6% to 1.4% polymer two phases form - a non-Newtonian supernatant solution containing ~0.6% polymer, and a clear, one-piece, flexible gel that takes the shape of its container as it forms and retains that shape for long times after removal from the vessel. The gel also retains the solvent even under moderate applied pressure. No such gel forms from HEC in either water alone or EtOH/water at these or higher polymer levels. Thus the gels which form from HMHEC must arise due to intermolecular interactions involving the hydrophobic side chains on the polymer. The polymer contents of the two phases are shown in Figure 4.5. These results show that the supernatant solution becomes saturated at a polymer level of 0.28 ± 0.02 g/50 ml, which is approximately equal to the concentration at which the gel first appears, while the remaining polymer goes into gel. Above 1.4% HMHEC the solutions were highly non-homogeneous and were therefore not investigated.

It is interesting to note that the volume of the gel phase is always equal to that of the supernatant, while the supernatant composition is always the same. Thus the gel is not an equilibrium phase. Nevertheless, results indicate that the rheological properties of the gel scale with total polymer content. It is significant that the solvent composition giving the "best" solution according to our definition also gives the strongest gels as discussed in chapter 5. This implies that the network structure is set

up in the solution phase before the gel precipitates. More details on the rheological characterization and interpretation of these results are given in chapter 5.

4.3 Properties of HMHEC Films

Clear, non-uniform solid films were prepared by drying HMHEC gels or concentrated HEC solutions in air at room temperature and then immersed in either pure water, 50% (v/v) ethanol/water, or pure ethanol. In both water and ethanol/water, the HMHEC films swelled isotropically to their original volumes without dispersing further, while the HEC films dispersed completely, forming viscous solutions. In pure ethanol, neither type of film dissolved or changed shape even after remaining in the ethanol for as long as five days. Both HEC and HMHEC are virtually insoluble in pure ethanol. It is clear that the even after removal of the original solvent, the hydrophobic aggregates in HMHEC networks are completely segregated from the bulk material and are stable to the drying process.

The films were investigated by DSC to determine whether the aggregates, which were shown to exclude both water and ethanol, were crystalline or amorphous. This information is important in the context of projected applications for these materials in which permeating solutes will be retained or released by the microdomains. Only amorphous aggregates

incorporate foreign material. Results showed no evidence of melting at 24°C, which is the melting point of 1-dodecanol. This was an appropriate control material since the side chains on the polymer are attached via an ether linkage to ethylene oxide units along the HEC backbone. We conclude the aggregates are amorphous and should be able to accommodate small solutes in their interiors.

4.4 Conclusions

We have seen that hydrophobic aggregates form which are composed of alkyl side chains from HMHEC. The number of side chains in each aggregate is high enough that the aggregates can exclude water, are stable to both oscillatory shear and swelling pressure, and remain intact even on drying. Thus these aggregates must be densely packed in an ordered array, although they are not crystalline. In these regards, they appear to resemble surfactant micelles. This opens the possibility that they may be able to solubilize small solutes and release them into the bulk polymer network at a steady rate.

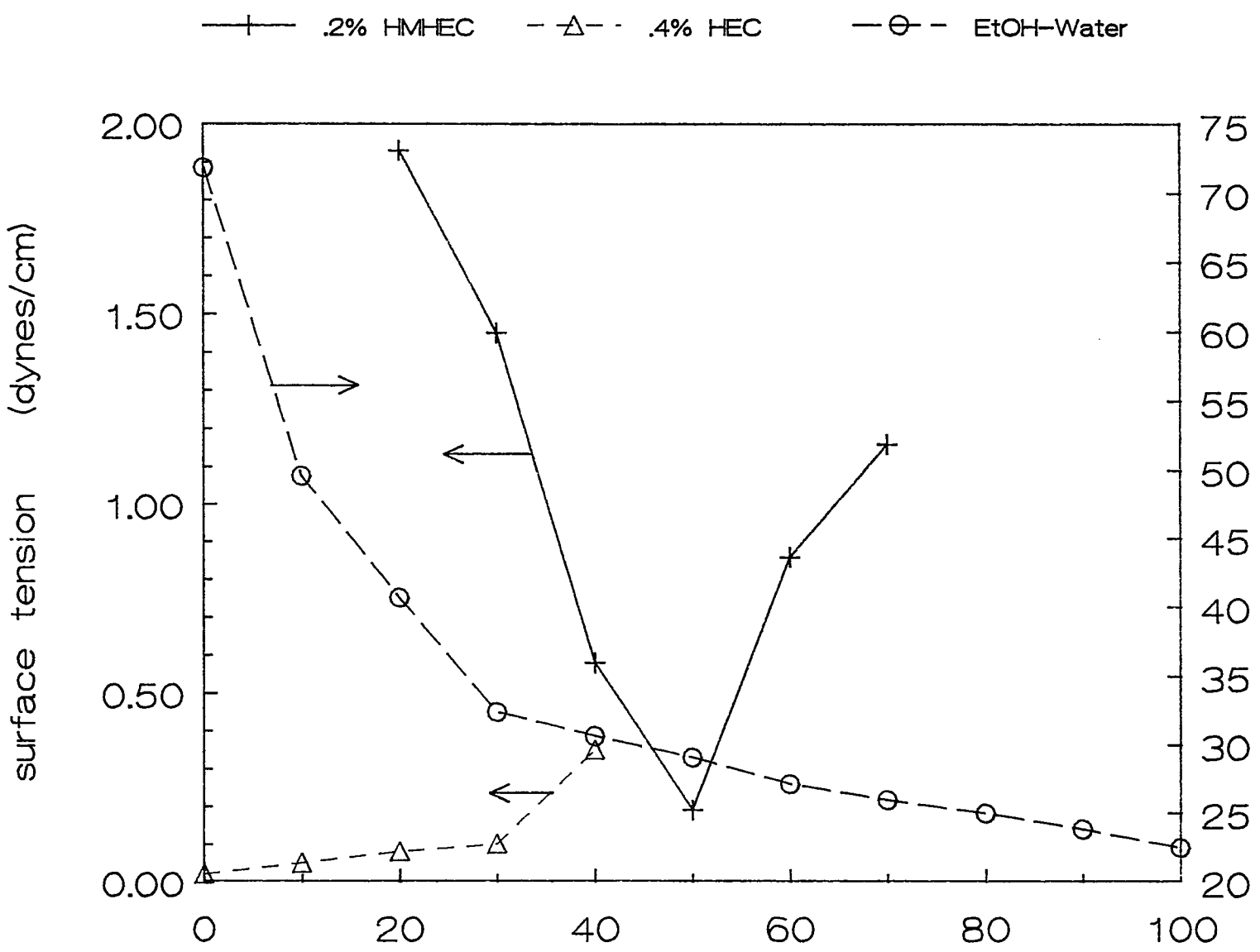

Figure 1 Volume % EtOH in EtOH–Water Solution

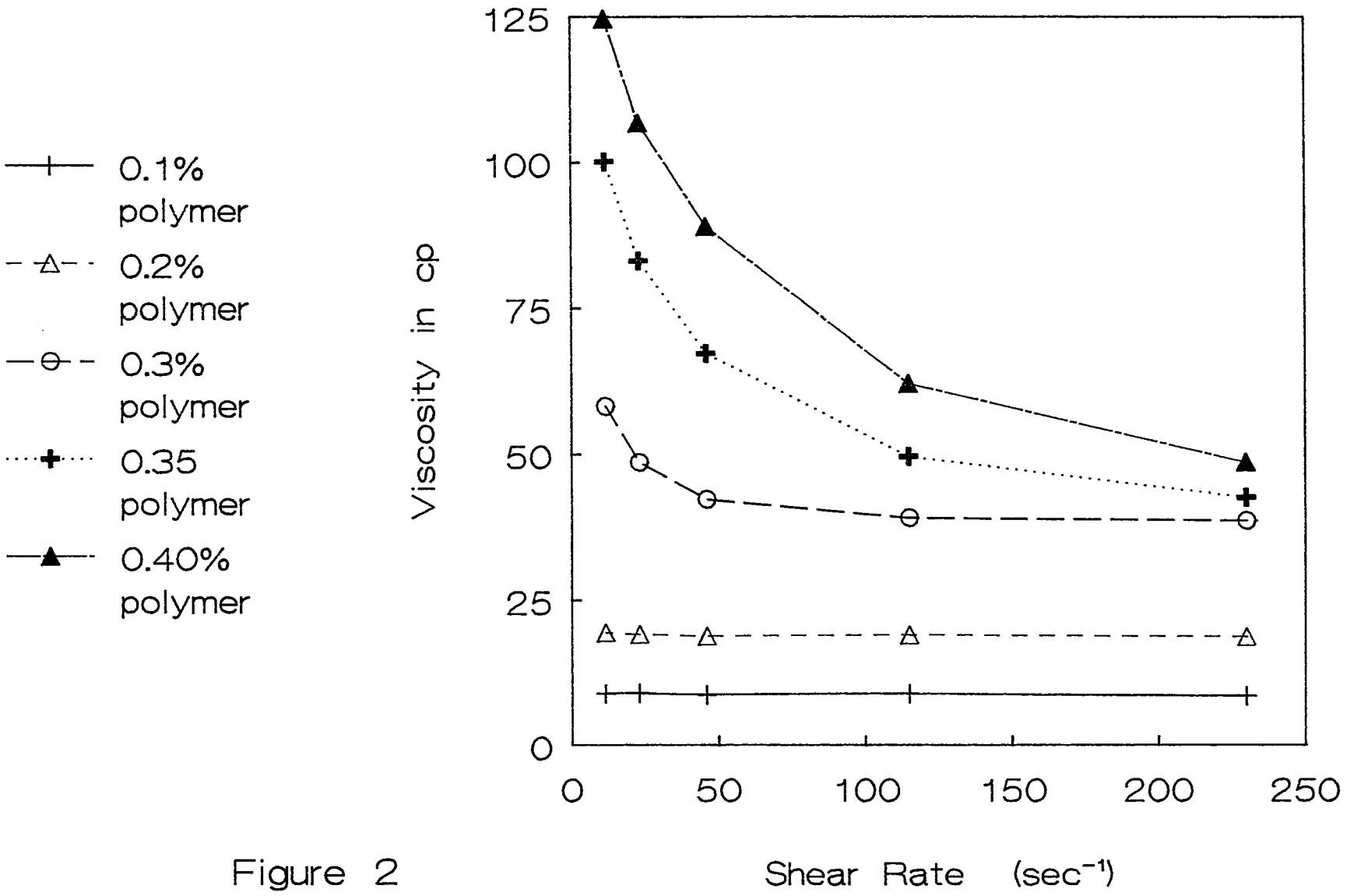
0.1% polymer
0.2% polymer
0.3% polymer
0.35 polymer
0.40% polymer
Viscosity in cp
125
100
75
50
25
0
0
50
100
150
200
250
Shear Rate (sec⁻¹)

Figure 2

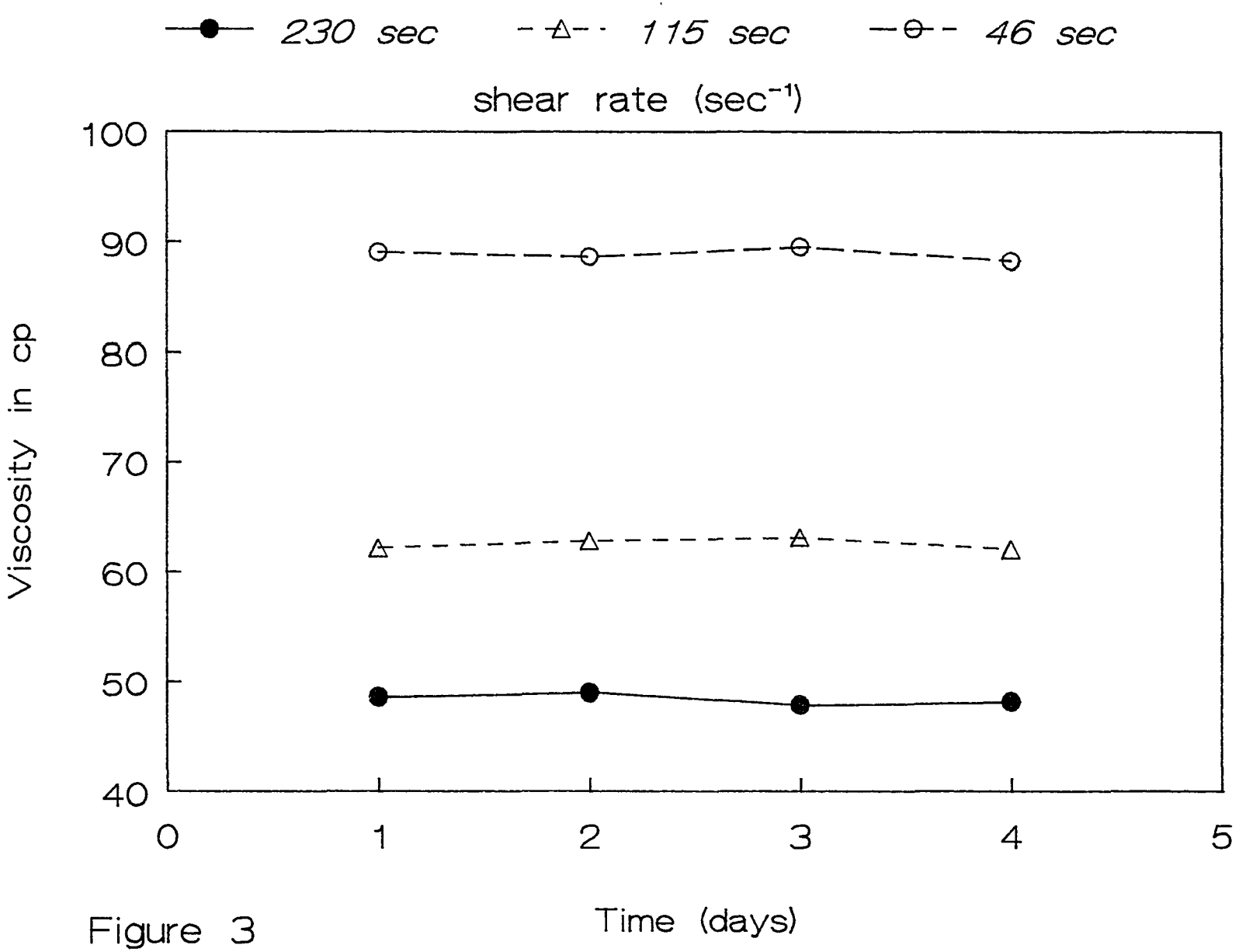
230 sec
115 sec
46 sec
shear rate (sec⁻¹)
Viscosity in cp
100
90
80
70
60
50
40
0
1
2
3
4
5
Time (days)

Figure 3

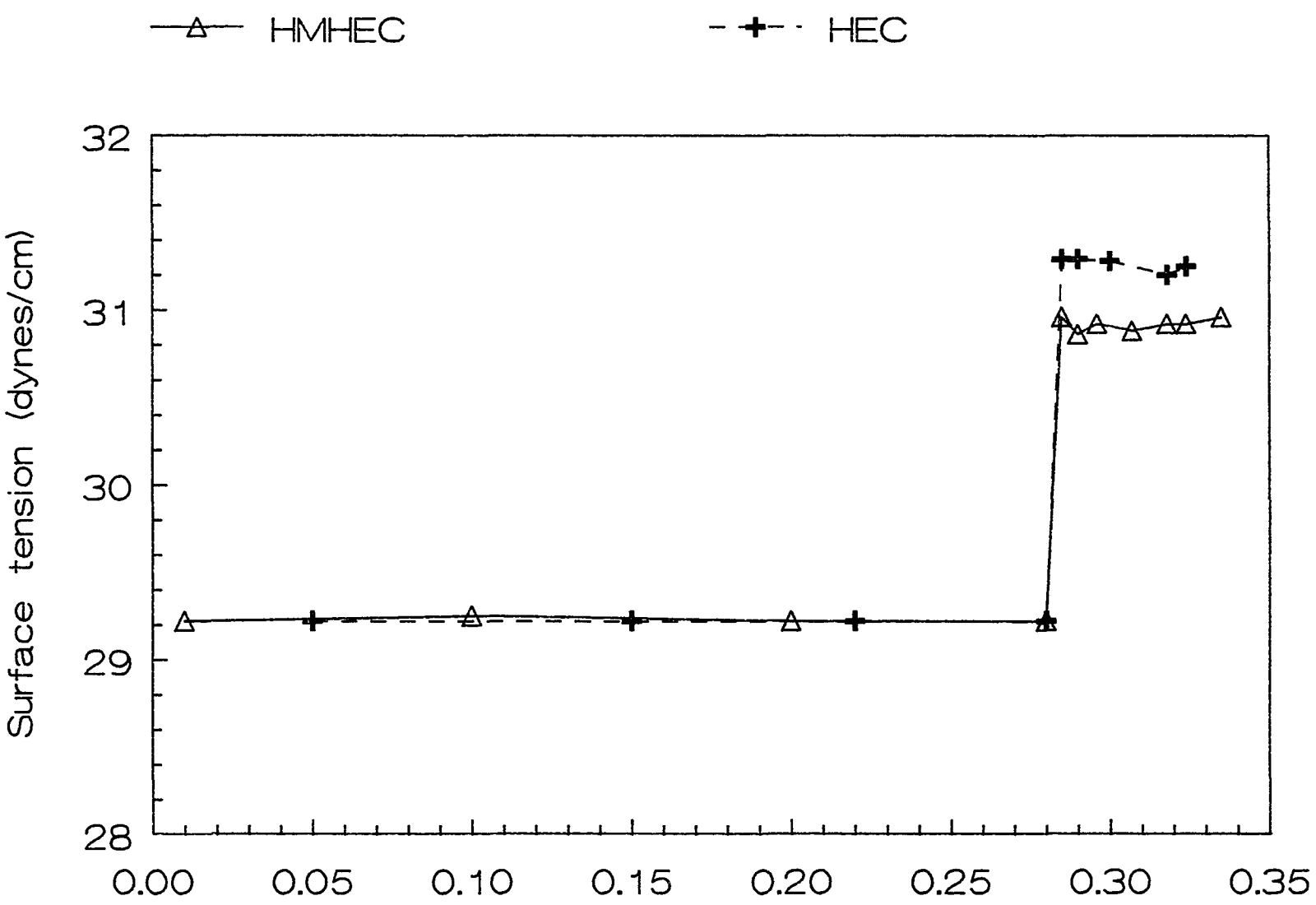
HMHEC
HEC
Surface tension (dynes/cm)
32
31
30
29
28
0.00
0.05
0.10
0.15
0.20
0.25
0.30
0.35
Polymer (wt %)

Figure 4

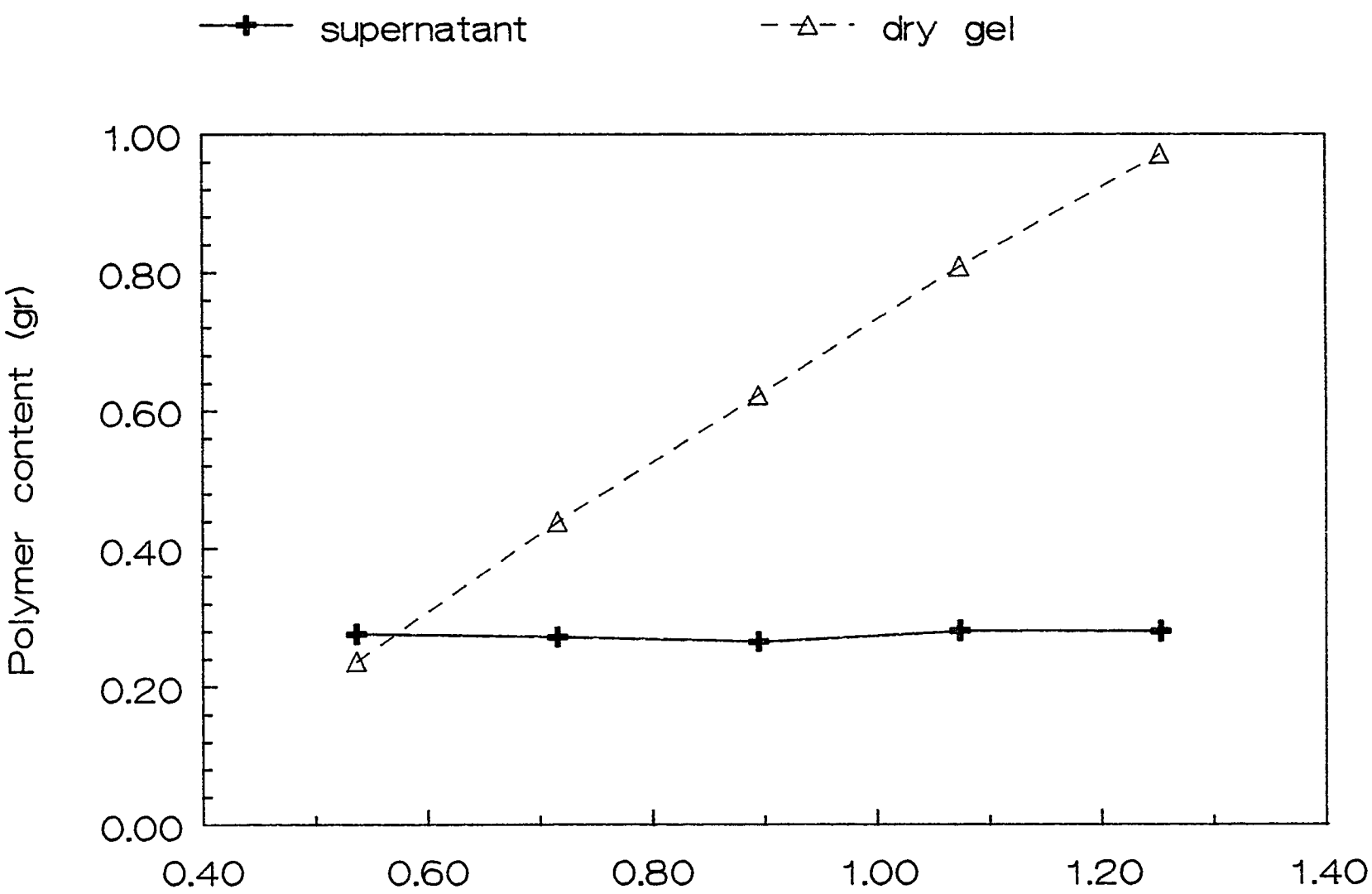
supernatant
dry gel
Polymer content (gr)
1.00
0.80
0.60
0.40
0.20
0.00
0.40
0.60
0.80
1.00
1.20
1.40
Starting amount of polymer (gr)

Figure 5

Chapter 5

BULK AND MICROSCOPIC PROPERTIES OF COPOLYMER NETWORKS IN MIXED AQUEOUS SOLVENTS

This Chapter contains the text of a manuscript describing results of the rheological and fluorescence characterization of HMHEC gels. The manuscript has been submitted to the Journal of Polymer Science: Part B: Polymer Physics, and is currently in review. Additional rheological and fluorescence data not included in the manuscript for publication are also presented in this chapter.

5.1 INTRODUCTION

The behavior of surface-active graft copolymers in aqueous solutions has been a subject of much interest and study by the authors (21,78) and others (35). It has been shown that these polymers self-associate in aqueous solutions, forming micelle-like aggregates consisting of water-insoluble side chains from the polymer. These aggregates may form either intra- or intermolecularly. The net effect of the latter process is the formation of hydrogels with dispersed hydrophobic microdomains.

The bulk and microscopic properties of dispersed-phase hydrogels are of interest from several standpoints. In the bulk, the microdomains serve as pseudo-crosslinks among several macromolecules. Thus the rheological properties of these gels are expected to resemble those of cross-linked materials over a finite range of applied shear stress. On a microscopic level, the microdomains will resemble surfactant micelles, with the ability to sequester solutes which are only sparingly soluble in the aqueous phase. This makes these gels of interest as media for separations technology and controlled release.

To date most of the work published on microphase separation in polymers has focused on block copolymers. The microphases are composed of segments of both types of

blocks, as expected from steric constraints on the polymer, but have higher concentrations of the insoluble segments closer to the center of the aggregates, as expected from solution thermodynamics. Structural properties of the polymer such as molecular weight, uniformity, chain flexibility, and stereoregularity of the blocks, as well as the polymer/solvent interaction parameter for each of the blocks in the solvent of interest, all contribute to the tendency for aggregate formation and the structure of the resulting aggregates. Solution properties of block copolymer solutions have been characterized experimentally using small angle neutron scattering (36) quasielastic light scattering (7), gel permeation chromatography, electron microscopy (20), fluorescence spectroscopy (13), and small angle X-ray scattering (13). Intrinsic viscosity studies have also been used to document the occurrence of hydrophobic interactions and microphase separation (12).

Krause (20) reviewed empirical evidence of the occurrence of microdomains in block copolymer membranes such as those used for reverse osmosis and ion exchange processes. Depending on whether they are dispersed or continuous, the microphases may either sequester compatible solutes or serve as channels for their transport through the membrane. Partitioning of solutes into the microdomains was found to be a complex function of solute structure and microdomain structure and composition and could not easily

be predicted quantitatively. Solid networks prepared as cast films from block copolymer solutions have been characterized using differential scanning calorimetry (DSC) (1,2) and electron microscopy (5). Microphase separation resulting in a dispersed-phase structure occurs even in the solid state above T_g (19), demonstrating that the dispersed-phase structure is the preferred configuration for these polymers in a network.

Relatively little work has been reported on microphase separation in graft copolymers. Graft copolymers represent an important class of network-forming surface-active polymers because they can be produced easily from synthetic and naturally-occurring homopolymers such as poly(vinyl alcohol), cellulose derivatives, etc. (4). The physical characterization of graft copolymers composed of alkyl side chains on a water-soluble backbone has been the subject of much study by the authors and it has been shown that in the presence of surfactants the grafts aggregate into microdomains resembling comicelles of uniform structure composed of both the hydrophobic side chains and surfactant molecules. Thus by modifying the solvent, and hence the interaction parameter,χ, these polymers can be driven to phase separate (18,24).

In this work, we present results of an investigation of dispersed-phase hydrogels formed from a surface-active graft copolymer in mixed ethanol/water solvents.

5.2 EXPERIMENTAL SECTION

The polymer used for this work is a water-insoluble hydrophobically modified hydroxyethyl cellulose (HMHEC) with molecular weight ~10^6. HMHEC is a graft copolymer whose backbone, hydroxyethyl cellulose (HEC), is a water-soluble cellulose derivative. Alkyl groups are grafted at random sites along the backbone, rendering the polymer insoluble in water. HEC with the same backbone molecular weight as the HMHEC used in these experiments was used as the control material, permitting us to identify those effects which are due exclusively to the presence of the side chains. In this study, HMHEC with a molar substitution (MS) of 3.8 ethylene oxide (EO) groups per anhydroglucose unit and a hydrophobe degree of substitution of 1.33% (w/w) alkyl grafts (corresponding to ~78 side chains per backbone) was used. Ethanol/water at various compositions was used as the solvent. Pyrene (Aldrich, 99% pure), was recrystallized twice from ethanol. Brij 30 surfactant ($C_{12}H_{25}(OCH_2CH_2)_4OH$) was obtained from ICI Americas, Wilmington, Delaware and used as received.

Ethanol/water mixtures with different compositions were prepared volumetrically by combining distilled water,

saturated with pyrene ($3x10^{-7}$), and appropriate amounts of ethanol. HMHEC was then added to the solvent by weight and stirred overnight at room temperature. At HMHEC concentrations > 0.6%, a supernatant solution and a gel were formed. The spectra of pyrene were obtained by exciting the solutions at 310 nm and recording the emission over the range 350-450 nm using a Spex Fluorolog-2 Model 112A Fluorescence Spectrophotometer (Spex Industries, Inc., Edison NJ). All spectral characteristics of pyrene remained constant for at least 2 days after preparation, indicating that the pyrene had equilibrated throughout the multiphase system.

Dynamic mechanical measurements of the gels were performed using a cone and plate Instron 3250 Rotary Rheometer operating in an oscillating mode. The frequency range of the instrument was from 0.6 to 100 rad/sec. The torque and phase angle were measured with a Solartron frequency response analyzer and the storage and loss moduli of the gels were obtained. Differential scanning calorimetry (DSC) studies were conducted using a Dupont Instruments TA2100 Thermal Analyzer and 910 DSC.

5.3 RESULTS

In order to produce copolymer networks such as those

described above, it is necessary first to solubilize the polymer in an appropriate solvent. By definition this means that all of the groups on the copolymer must be compatible with the solvent. Then the solution conditions must be adjusted so as to drive the hydrophobic moieties into clusters, or microdomains.

Ethanol disrupts aqueous phase hydrophobic interactions by breaking the structure of the water, allowing non-hydrogen bonding species to become solubilized. Thus ethanol/water solutions are appropriate solvents for HMHEC. The solubility of the polymer and the resulting solution and gel properties will depend on the composition of the EtOH/water solvent. We define the optimum solvent composition as the composition in which the side chains are maximally exposed to the solvent, and hence to each other, thus allowing them to associate. This corresponds to the solvent composition in which the polymer exhibits the lowest tendency to adsorb at the solution interface. We have shown using surface tension measurements that a 50% (v/v) ethanol-water solution corresponds to the "best" solvent for the polymer. Using this solvent, polymer solutions become saturated at 0.6% HMHEC, and at > 0.6% two phases form - a non-Newtonian supernatant solution and a clear, one-piece, flexible gel that retains the shape of its container even on removal and retains solvent even under moderate applied

pressure. When gels were made from 100 cm^3 of starting solution containing > 0.6% HMHEC, the volume of the gel phase was always ~50 cm^3, regardless of total polymer content of the gel, and the supernatant was always a saturated 0.6% solution. Thus the gel phase is not in equilibrium with the supernatant, rather it is a precipitate. No such gels form from HEC in either water alone or EtOH/water at these polymer levels. Thus the gels which form from HMHEC must arise due to intermolecular interactions involving the hydrophobic side chains on the polymer.

Investigation of these interactions was carried out using steady state fluorescence measurements with pyrene as a probe. The relative intensities of the vibronic bands of pyrene reflect the hydrophobicity of the probe's environment, as follows. The emission spectrum of pyrene in the frequency range specified above is characterized by five distinct peaks. The ratio of the third to the first peak (I_3/I_1) is an inverse function of the polarity of the pyrene's environment (24). Because pyrene itself is relatively non-polar, we expect it to partition into any hydrophobic regions that may be present. Typical spectra obtained from our gels are shown in Figure 5.1. It can be seen that the peak height ratio varies significantly comparing the spectra of the gel and the corresponding

solvent.

Relative hydrophobicities, as indicated by I_3/I_1, of representative gels and control solutions are shown in Figure 5.2. The peak height ratio of pyrene in the solvent alone increases linearly with ethanol concentration from 0.6 in pure water to 0.88 in pure ethanol. HEC at a concentration of 0.1% by weight raises the hydrophobicity of water-rich solutions, but has a negligible effect above 40% ethanol. By contrast, 0.1% HMHEC produces a greater increase in the solution hydrophobicity, and the effect is evident at ethanol concentrations up to 70%. It is important to note that this effect is not due solely to the presence of the hydrophobic side chains, since control solutions containing HEC and Brij 30 surfactant, whose chemical composition is similar to that of the side chains, do not differ significantly from solutions with HEC alone. The results shown on this figure are for HEC solutions containing Brij 30 at a level 10 times higher than the substituent level on the equivalent amount of HMHEC (but still below the critical micelle concentration (cmc) of the surfactant in water). Thus we have evidence of the presence of hydrophobic regions even in dilute HMHEC solutions.

The I_3/I_1 values for HMHEC gels are significantly higher than those of the corresponding solvents or of any of

the control solutions. This demonstrates that there are distinct hydrophobic regions in the gels which are not present in the solutions and whose existence and composition are relatively insensitive to the bulk solvent composition. While it is clear that these regions are made up of side chains from the polymer, it is not possible from these experiments to determine their exact composition. The I_3/I_1 ratio for Brij 30 micelles in water is 0.92, which is higher than the value in our gels (0.84). However, some of the pyrene in our gels remains in the bulk (aqueous) due to its solubility in ethanol. Thus the I_3/I_1 ratio, which reflects the average hydrophobicity of the pyrene environment, will have a significant contribution from the aqueous phase.

Figure 5.3-5.8 show frequency dependence of the storage and loss moduli (G' and G", respectively) of HMHEC gels in 50% ethanol. It can be seen that the moduli increase as the polymer concentration in the gel increases. This behavior is summarized in Figure 5.9, showing the frequency dependence of the storage modulus alone for various polymer concentrations. At long times, i.e. low frequencies, the hydrophobic linkages break up, giving rise to a steep drop in the storage and loss moduli. At higher frequencies, the linkages are relatively stable, but still somewhat sensitive to applied shear and the spectra become relatively flat. We can use values of G' from both ends of this pseudo-plateau

region to obtain information about the structure of the networks. Figure 5.10 shows the effect of solvent composition on the storage modulus of HMHEC gels. The value for G' at 30 rad/sec, which is near the low frequency end of the pseudo-plateau, is plotted as a function of ethanol concentration in Figure 5.11. There is a distinct peak in this function at 50% (v/v) EtOH, corresponding to the concentration where the surface activity of the polymer in the solution was at a minimum (1). The effect of polymer concentration on the storage modulus at 30 rad/sec is shown in Figure 5.12. By analogy with permanent networks we used this value, G'_{30}, to calculate the molecular weight between linkages, M_l, in our system, using the equation:

$$M_{l,30} = \frac{\rho \phi RT}{G'_{30}} \tag{5.1}$$

where ρ is the density of dry polymer, ϕ is the volume fraction of the polymer in the solution, R is the universal gas constant, and T is the absolute temperature of the sample. The molecular weight between linkages gives the number of linkages per polymer chain, N, by :

$$N = \frac{MW}{M_l} \tag{5.2}$$

where MW is the molecular weight of the polymer. The average value using G'_{30} is N_{30}, and is equal to 22.8 ± 1.3 linkages per backbone or ~29% of all the side chains on the HMHEC used here. Results are summarized in Table 5.1. At

higher frequencies, G' goes up, indicating that the linkages are more stable. At 50 rad/sec, N_{50} = 26.2 ± 1.5, or ~34% of all the side chains are in intermolecular linkages.

In an effort to determine the stability and the physical nature of the microdomains which are the structural components of these networks, we conducted swelling and calorimetry experiments on dried HMHEC films. The films which form when HMHEC/EtOH/water gels are dried in air are smooth, clear and rather rigid. By contrast, when concentrated HEC/water solutions are dried in air a granular film results which has very low mechanical integrity. Both types of films were reconstituted in either pure water, 50% (v/v) ethanol/water, or pure ethanol. In both water and ethanol/water, the HMHEC films swelled isotropically to their original volumes without dispersing further, while the HEC films dispersed completely, forming viscous solutions. In pure ethanol, neither type of film dissolved or changed shape even after remaining in the ethanol for as long as five days. However, both HEC and HMHEC are virtually insoluble in pure ethanol. It is clear that the even after removal of the original solvent, the hydrophobic aggregates in the HMHEC networks are segregated from the bulk material and are stable to the drying process.

The films were investigated by DSC to determine whether

the aggregates, which were shown to exclude both water and ethanol, were crystalline or amorphous. This information is important in the context of projected applications for these materials in which permeating solutes will be retained or released by the microdomains. Only amorphous aggregates can incorporate foreign material. Results showed no evidence of melting at or near 24°C, which is the melting point of 1-dodecanol. This was an appropriate control material since the side chains on the polymer are attached via an ether linkage to ethylene oxide units along the HEC backbone. We conclude the aggregates are amorphous and should be able to accommodate small solutes in their interiors. Additional evidence for this is provided by the result that pyrene partitions into hydrophobic regions in the gel. The fact that ethanol is not sequestered by the aggregates thus reflects ethanol's high solubility in water rather than a tendency for the microdomains to exclude small molecules.

5.4 DISCUSSION

It is significant that the solvent composition giving the "best" solution according to our surface tension results also gives the strongest gels. This implies that the network structure is set up in the solution phase, where the polymer is maximally solubilized, before the gel precipitates. Furthermore, the hydrophobic clusters are composed exclusively of side chains from the polymer. This

was concluded based on dialysis experiments which showed that when HMHEC solutions and gels are dialyzed against EtOH/water (60% v/v EtOH), the bathing solution does not become depleted of ethanol even after several days. Thus the sole function of the ethanol appears to be to facilitate contact among the side chains in the starting solution, that is, to reduce the polymer-solvent interaction parameter. This differs from our results on HMHEC gels formed from surfactant solutions, in which the surfactant molecules are actually an integral component of the microdomains (1-3).

We can gain additional insight into the nature of the microdomains from the fact that M_l at a given frequency is a constant for all polymer concentrations. For this particular polymer, the percentage of side chains included in intermolecular linkages ranges from 29% to 34% over the frequency range 30-50 rad/sec. However, it is not necessarily the case that the remaining side chains are free in the bulk phase. The side chains may also aggregate intramolecularly, which would not affect G'. It is likely that the microdomain formation in these networks is a process analogous to micellization in surfactant solutions, where the bulk phase becomes saturated with unaggregated side chains, and the remaining side chains are driven to aggregate, either inter- or intramolecularly. We speculate that the microdomains are characterized by an optimum

aggregation number and the total number of microdomains in the gel scales with total side chain concentration.

The pyrene experiments demonstrated that small solutes can indeed be sequestered by the microdomains in these hydrogels. Moreover the structural integrity of the microdomains depends on applied shear stress, suggesting that the rate of release of incorporated solutes may be manipulated by the application of external stress. These properties make these gels of potential importance in controlled release and separations applications. It remains to discover the limits on size and solubility of non-polar solutes for use with these materials.

ACKNOWLEDGMENTS

The authors would like to thank Dr. John Denuzzio for his contribution to this work. This work was supported by Aqualon Co. and PSC CUNY Grant No. 668309.

TABLE 5.1

SUMMARY OF RHEOLOGICAL RESULTS

weight percent HMHEC	volume fraction of polymer in gel, ($x10^3$)	storage modulus, $G'_{30,}$ (dynes/cm^2) $x10^{-3}$	$M_{l,30}$ ($x10^{-4}$)	number of linkages per chain ($N = MW/M_l$) (ω=30 rad/sec)
0.6	0.79	2.61	4.5	22
0.7	1.18	4.27	4.1	24
0.8	1.47	4.63	4.7	21
0.9	1.75	6.11	4.3	23
1.0	2.10	8.48	4.1	24

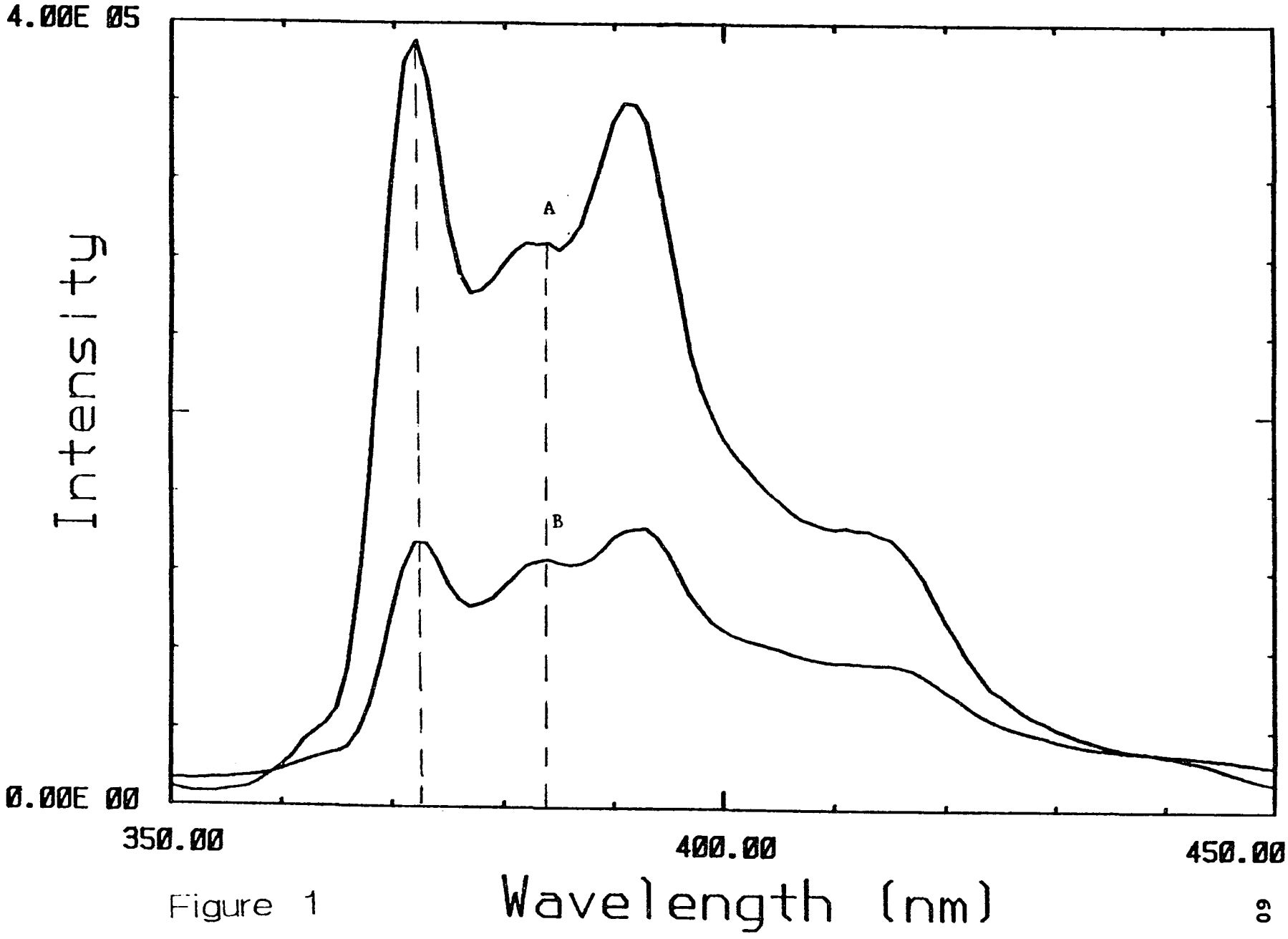
4.00E 05
Intensity
0.00E 00
A
B
350.00
400.00
450.00
Wavelength (nm)

Figure 1

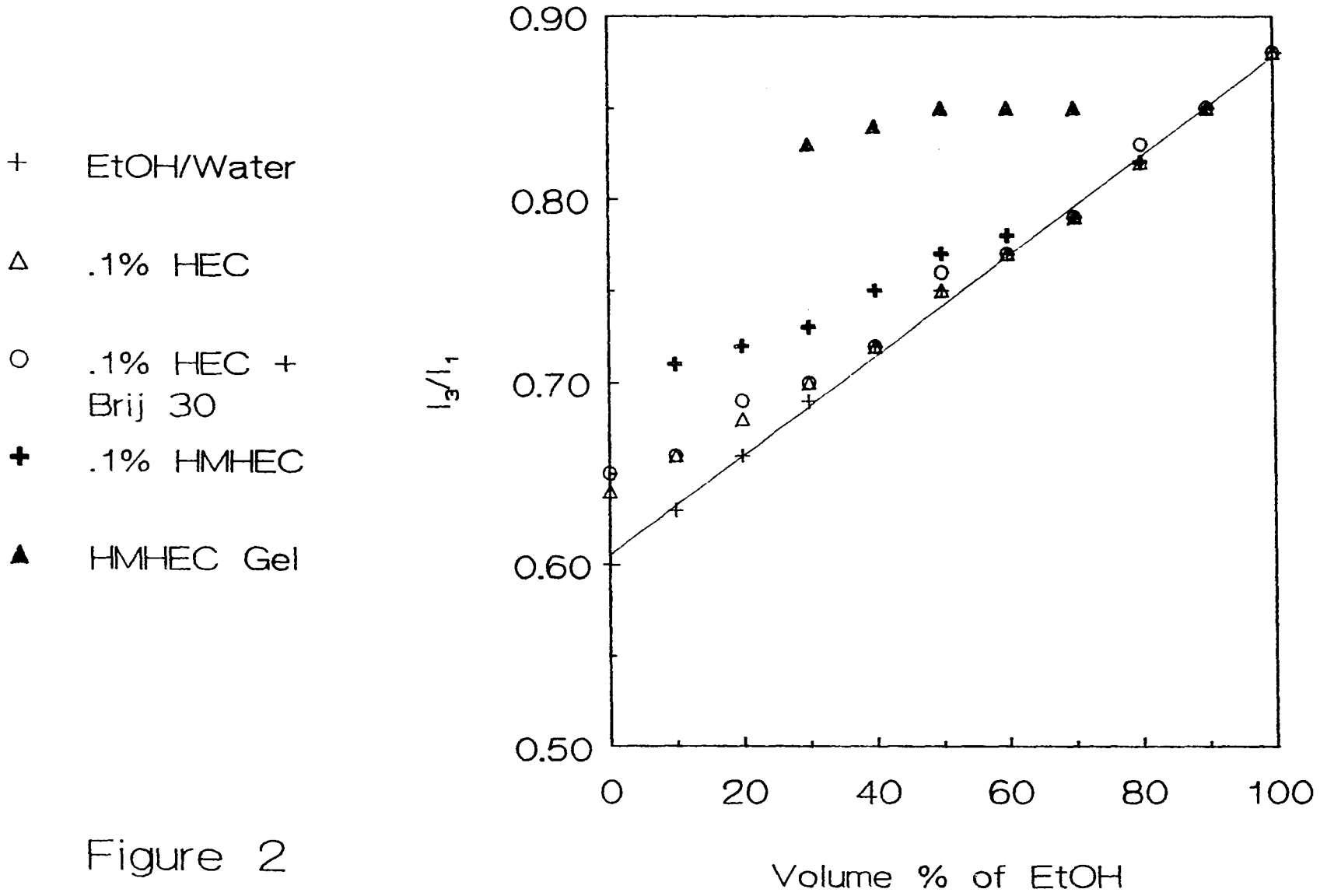
+ EtOH/Water
△ .1% HEC
○ .1% HEC + Brij 30
✚ .1% HMHEC
▲ HMHEC Gel
0.90
0.80
0.70
0.60
0.50
I_3/I_1
0
20
40
60
80
100
Volume % of EtOH

Figure 2

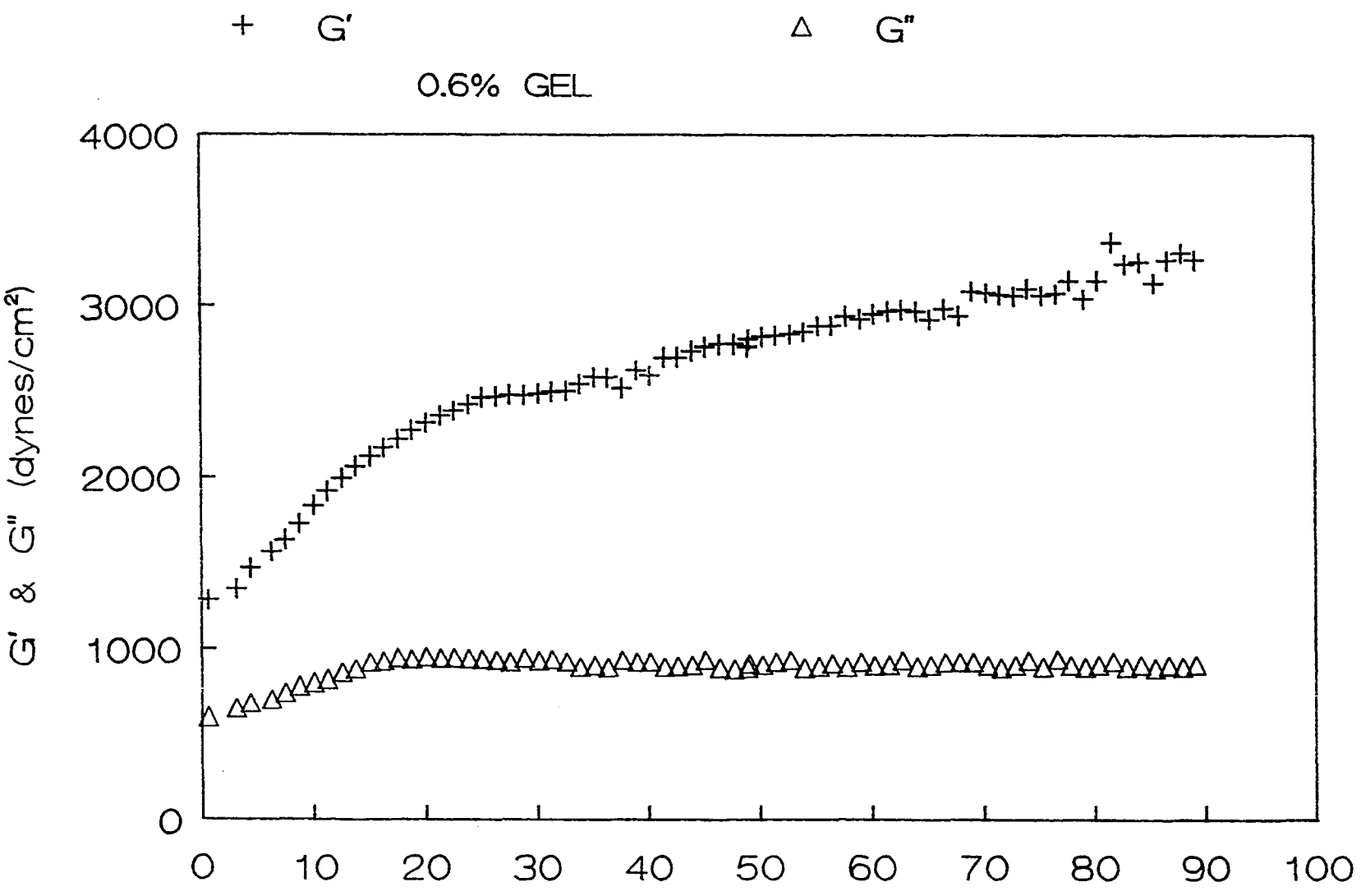
+ G'
Δ G"
0.6% GEL
4000
3000
2000
1000
0
G' & G" (dynes/cm²)
0
10
20
30
40
50
60
70
80
90
100
Angular Frequency (rad/sec)

Figure 3

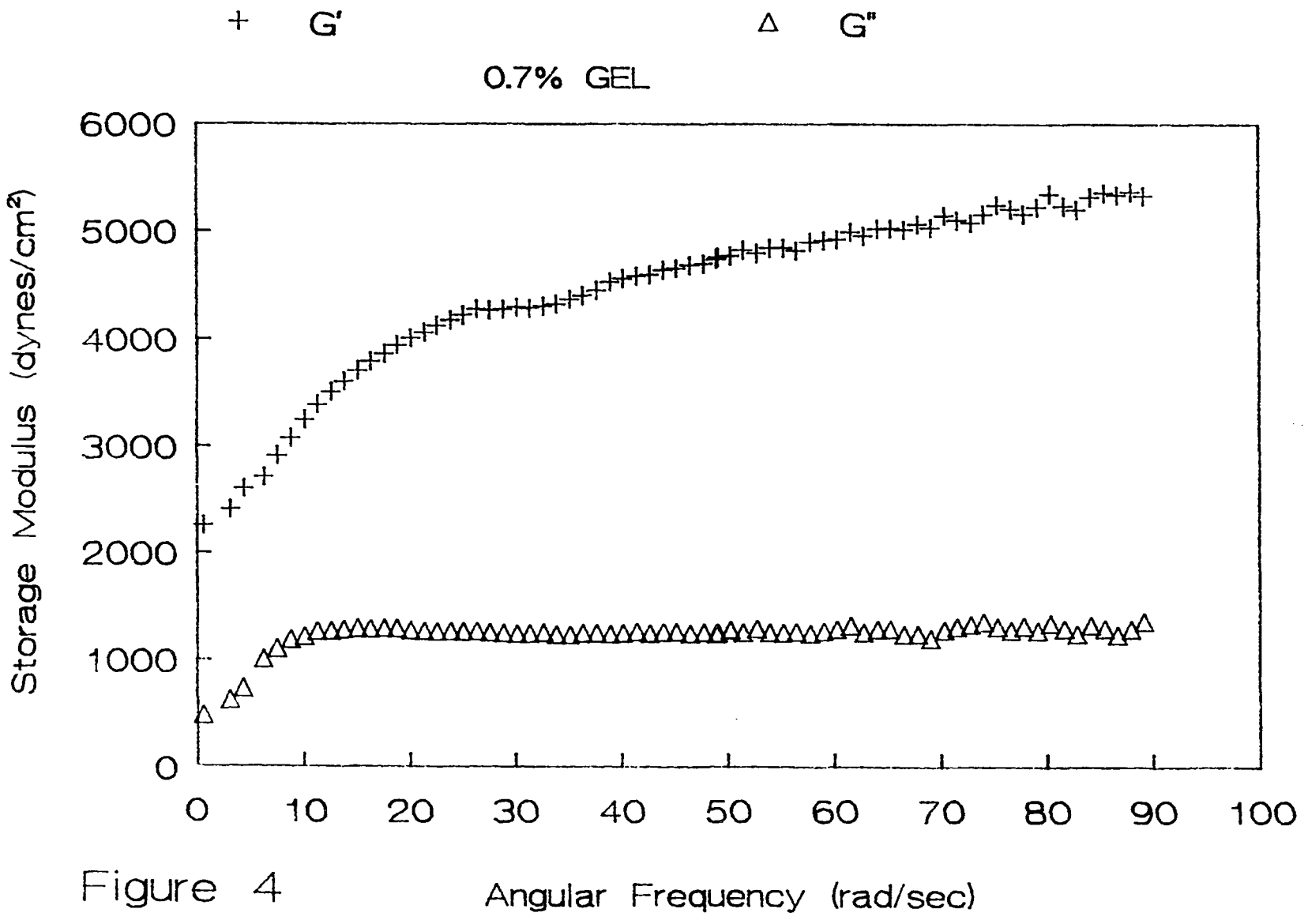
+ G'
Δ G"
0.7% GEL
Storage Modulus (dynes/cm²)
6000
5000
4000
3000
2000
1000
0
0
10
20
30
40
50
60
70
80
90
100
Angular Frequency (rad/sec)

Figure 4

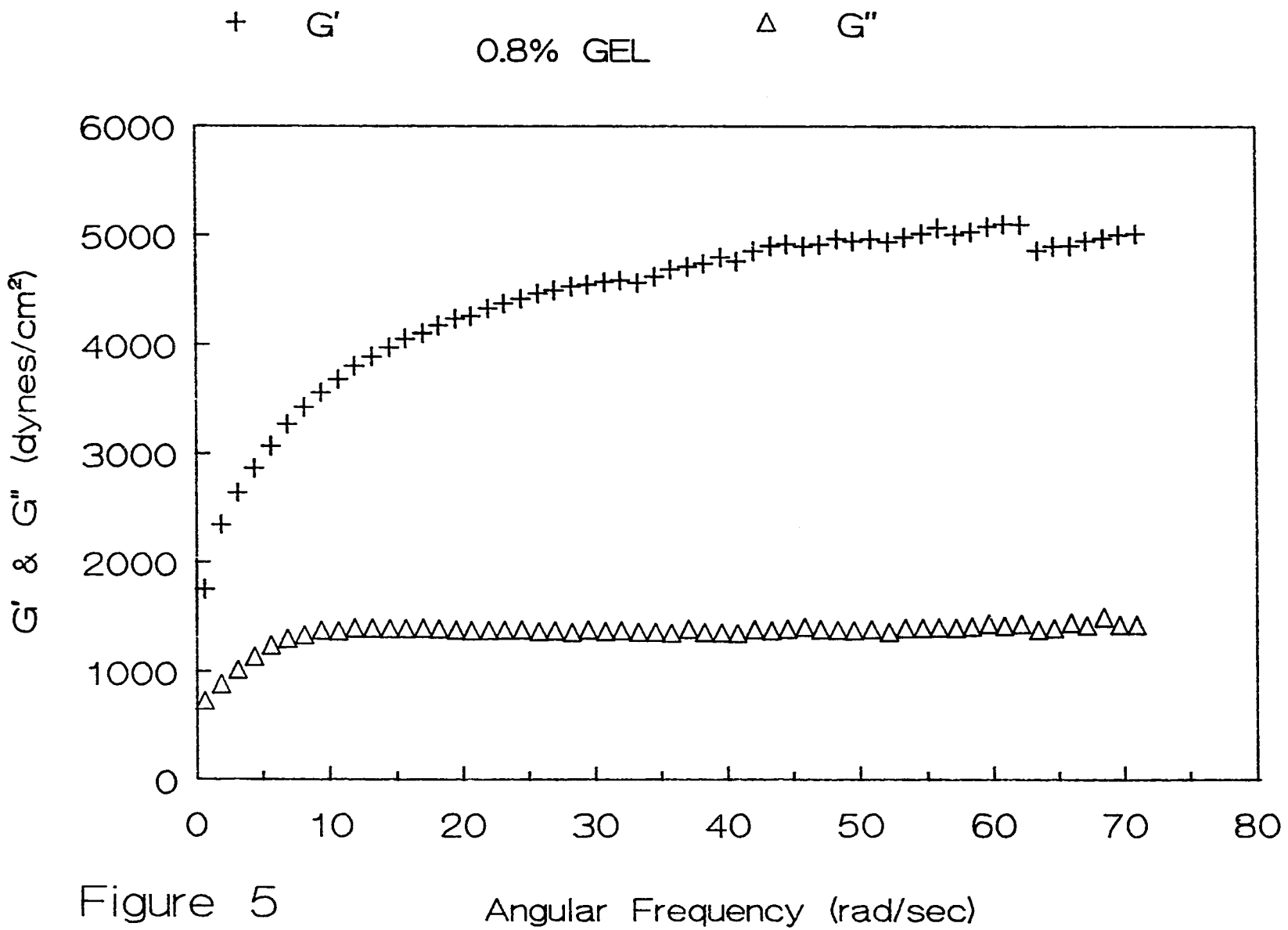
+ G'
Δ G"
0.8% GEL
6000
5000
4000
3000
2000
1000
0
G' & G" (dynes/cm²)
0
10
20
30
40
50
60
70
80
Angular Frequency (rad/sec)

Figure 5

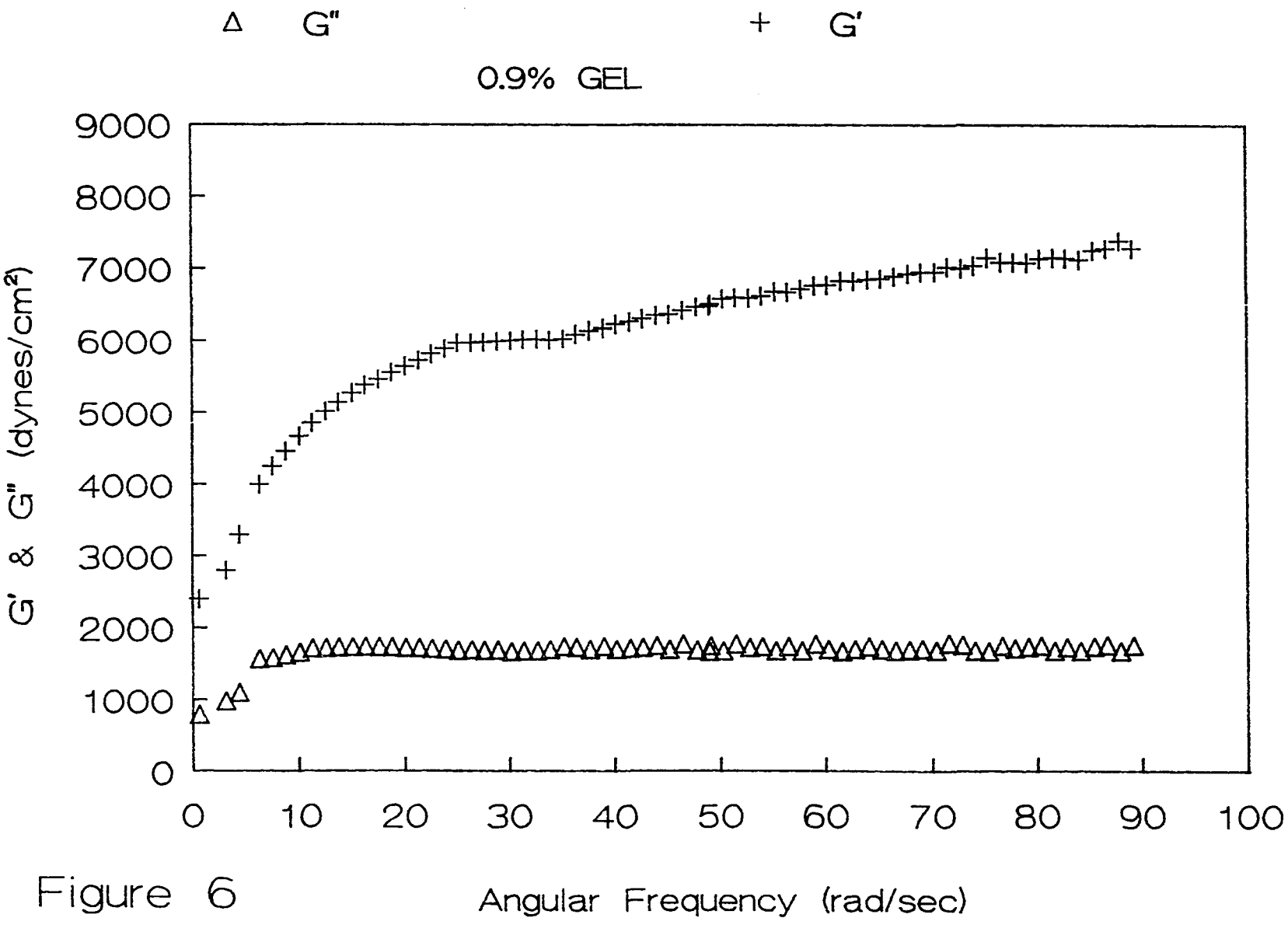
Δ G"
+ G'
0.9% GEL
G' & G" (dynes/cm²)
9000
8000
7000
6000
5000
4000
3000
2000
1000
0
0
10
20
30
40
50
60
70
80
90
100
Angular Frequency (rad/sec)

Figure 6

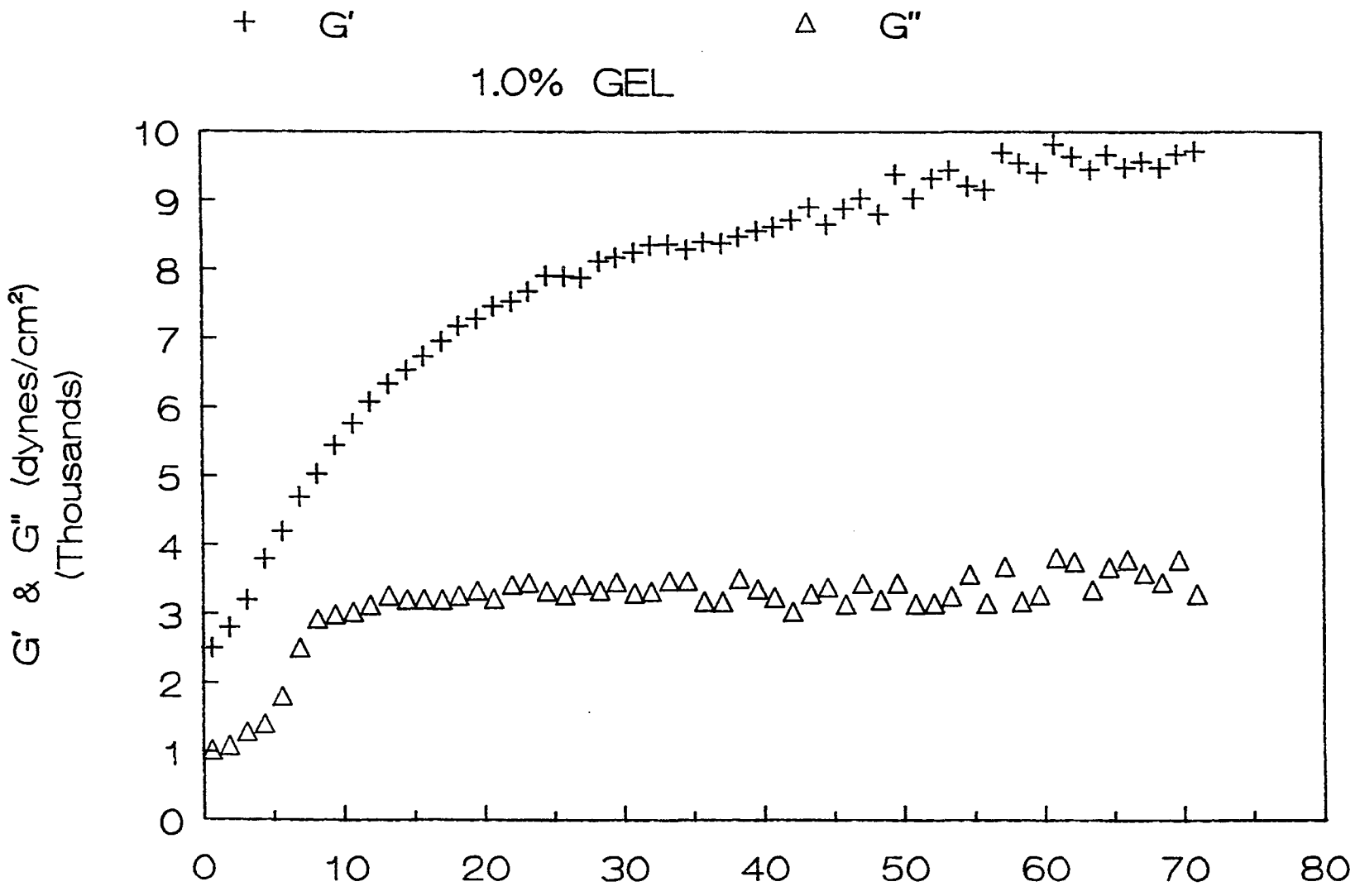
+ G'
Δ G"
1.0% GEL
G' & G" (dynes/cm²)
(Thousands)
0
1
2
3
4
5
6
7
8
9
10
0
10
20
30
40
50
60
70
80
Angular Frequency (rad/sec)

Figure 7

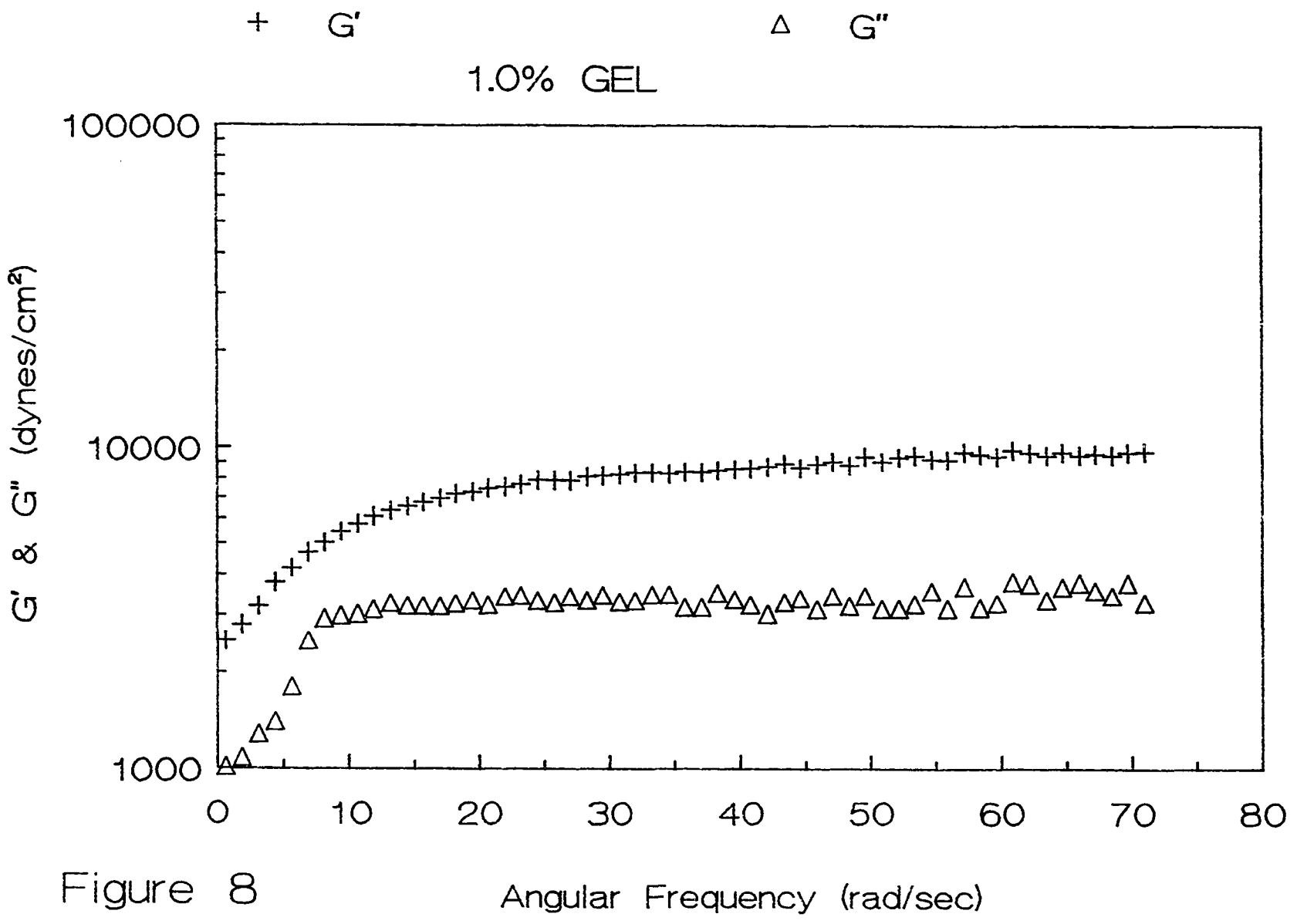
+ G'
Δ G"
1.0% GEL
100000
10000
1000
G' & G" (dynes/cm²)
0
10
20
30
40
50
60
70
80
Angular Frequency (rad/sec)

Figure 8

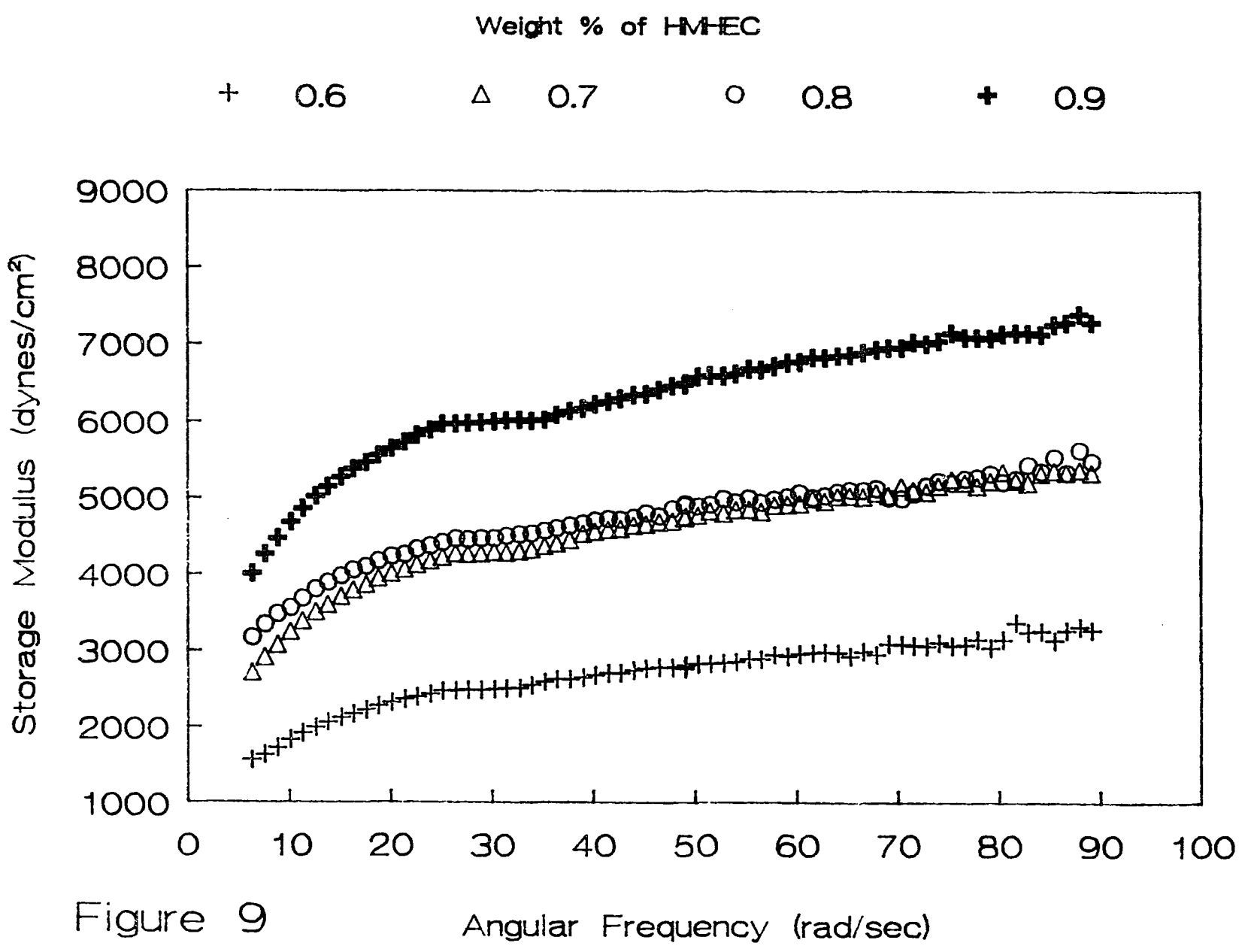
Weight % of HMHEC
+ 0.6
Δ 0.7
o 0.8
+ 0.9
Storage Modulus (dynes/cm²)
9000
8000
7000
6000
5000
4000
3000
2000
1000
0
10
20
30
40
50
60
70
80
90
100
Angular Frequency (rad/sec)

Figure 9

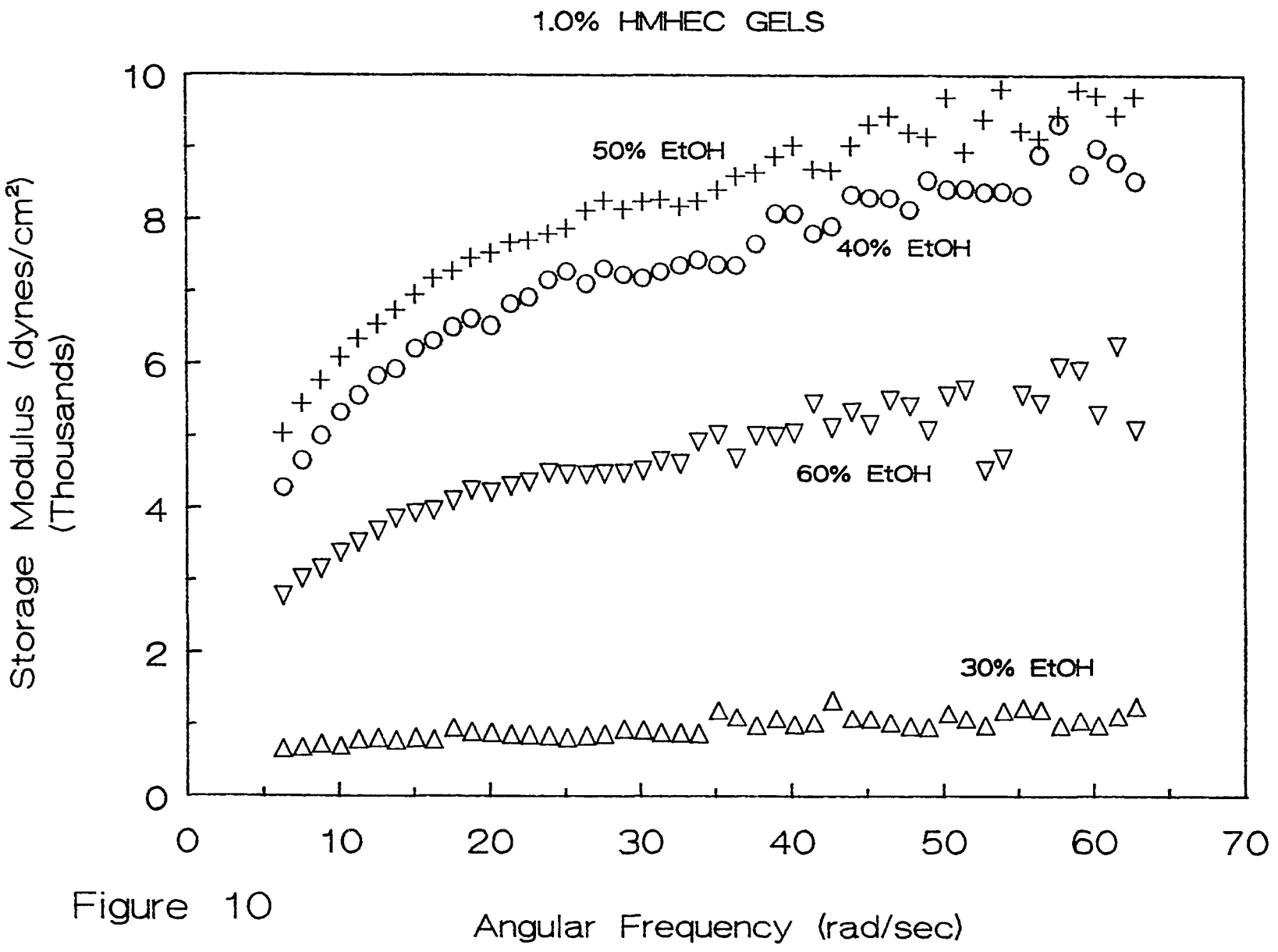
1.0% HMHEC GELS
Storage Modulus (dynes/cm²)
(Thousands)
10
8
6
4
2
0
0
10
20
30
40
50
60
70
50% EtOH
40% EtOH
60% EtOH
30% EtOH
Angular Frequency (rad/sec)

Figure 10

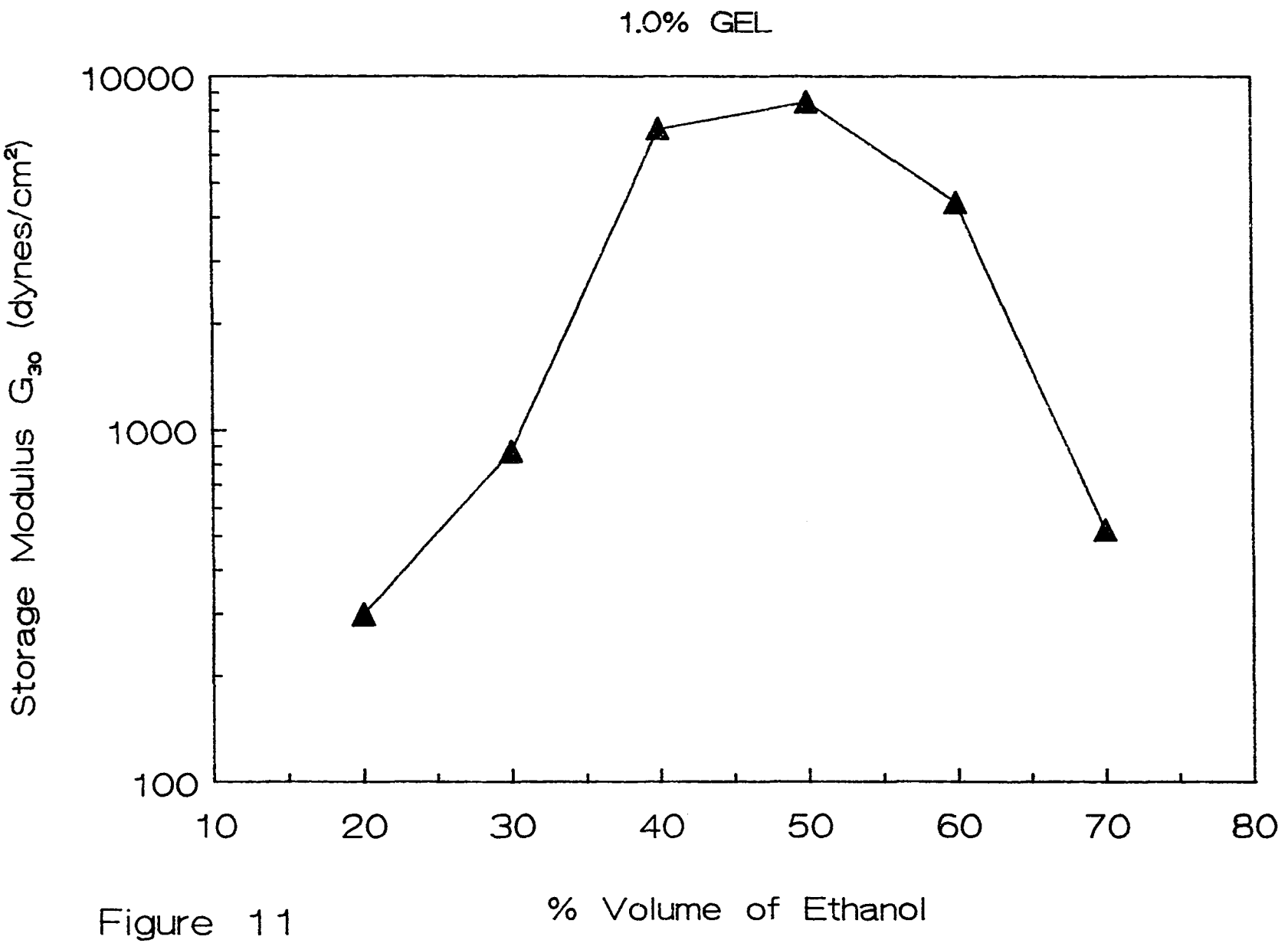
1.0% GEL
10000
1000
100
Storage Modulus G_{30} (dynes/cm²)
10
20
30
40
50
60
70
80
% Volume of Ethanol

Figure 11

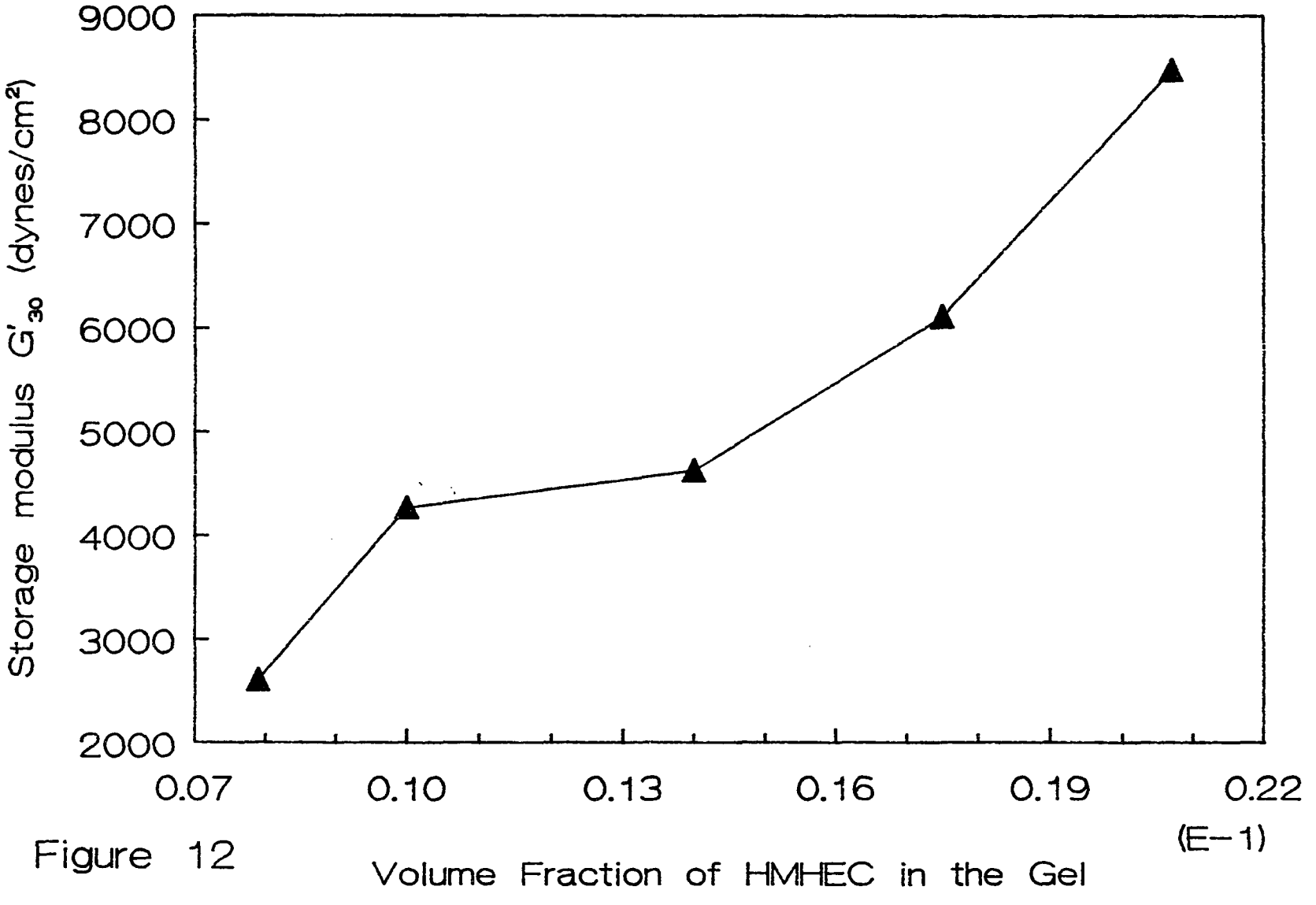
9000
8000
7000
6000
5000
4000
3000
2000
Storage modulus G'_{30} (dynes/cm²)
0.07
0.10
0.13
0.16
0.19
0.22
(E−1)
Volume Fraction of HMHEC in the Gel

Figure 12

Chapter 6

TRANSPORT PROPERTIES OF THE HYDROGELS-PRELIMINARY STUDIES

This chapter includes results of some preliminary experimental studies on the uptake and release of tryptophan and theophylline as well as a sketch of the mathematical model we will ultimately use to predict the release behavior of our gels from their structure. The model consists of the development of the governing equations describing mass transport within and out of the gels, as well as the solution of these equations. It still remains to solve the equations numerically to obtain concentration profiles of solutes as a function of gel structure.

6.1 Solute Uptake by Gels

The procedure for these experiments is described in section 3.5. There are two objectives in conducting these experiments. First we have studied the solute-loading process in the gels and second we have investigated their release properties. The first study is discussed in this section.

The solute-loading process was studied using as model two solutes (tryptophan and theophylline). We wanted to test the hypothesis that the solutes would absorb into the gels at a higher level than water. The total grams of solute in the gel were calculated by subtracting the grams of solute remaining in the soak solution after the gel was removed, from the grams in the starting saturated solution. The concentration of solute in each gel was found from the total grams of solute in the gel and the gel volume. The saturation concentrations of tryptophan and theophylline in water at 25°C were 11.4 and 7.0 g/L respectively. After the gels were removed the average concentration of the corresponding remaining soak solutions were 9.8 ± 0.3 and 6.2 ± 0.2 g/L. For tryptophan, at 25°C, we get an average of 73 ± 3% higher concentration in the gel than in saturated water solution, and for theophylline the average is 50 ± 7% higher. These results (table 6.2) have shown that the solutes appear to partition into the microdomains. It is important to note that this is a preliminary study with only few gels tested.

6.2 Release Studies

The release experiments were conducted using two different methods. First the swollen gel was immersed in 100 ml of distilled water and the cumulative concentration over time was measured using the calibration curves (Figure 6.1). The experiments were performed at two different temperatures, in order to investigate the integrity of the gels. Results for tryptophan and theophylline are plotted in Figures 2 and 3 respectively. We present the % solute released (M_t/M_∞ x100) over time, where M_t is the cumulative amount of solute in the solution at any time and M_∞ is the total solute loaded into the gel. As we can see from the results the effect of temperature on the release is not significant. The result is important because it indicates that there is no break up in the structure of the gels at least up to 40°C. The hydrophobic linkages that have formed as discussed in chapter 5 remain intact. If there was a change in structure, the release pattern would be different at the two temperatures. In addition from figures 2 and 3 we observed that the release was nearly constant for approximately the first 8 hours for tryptophan and for the first 10 for theophylline. The concentration of tryptophan and theophylline in the gels at the point where the release rate starts to level off (Fig. 2 and 3), is approximately 13.9 and 6.5 g/L respectively, which is near the saturation concentration of each solute in water. At longer times and for period of two days the concentration kept

increasing before it reached a plateau value. After that the concentration did not change, an indication that an equilibrium state had been reached between the remaining drug in the gel and the released drug. The total amount of tryptophan and theophylline released was 48% and 52% of the initial drug loading respectively.

The second method used in the experiments was to measure the concentration of the released solute in 100 ml of distilled water every hour and then replace the solution by equal amount of fresh distilled water. The reasoning is that in real applications when the drug is released in the human body, it is always convected away by flowing blood. Thus we wanted to investigate if and over how many hourly intervals the amount of released material remains constant. Figure 4 presents the actual grams of solute water released in 100 ml of water as a function of the number of intervals. Results show that the amount of tryptophan released remains nearly constant for three time intervals while that of theophylline for four. The concentration of tryptophan and theophylline in the gels at the end of the constant release was 12.9 and 7.5 g/L, which are close to the saturation concentrations in water.

6.3 Discussion

The release experiments have provided us with some

valuable information about our new materials. We have seen that the gels have a significantly higher capacity than water for the solutes, presumably due to partitioning into the microdomains. Moreover the release of these solutes remains constant for 8-10 hours. The period that the release remains constant as well as the maximum cumulative % released are very important. For example, controlled drug release applications one should try to maximize the released amount of drug from the device so that the drug is not wasted. Also is important that the release remains constant over long times so that continuous refilling of the device with drug is not needed. Other investigators have reported constant release from their materials for up to two weeks (83,88). For theophylline constant release has been reported for 12 hours (87) and 90% of the initial amount was released. Our results are promising because we believe that the period of constant release may be improved. From all the experiments we have seen that at the point which the release starts to flatten, the concentration of solute in the gels is near the saturation concentration of solutes in water. It appears that at that point most of the solute has been depleted from the microdomains. Thus by increasing the number of microdomains in the gel, we will be able to increase the uptake of the gels. We have seen from chapter 5 that the number of microdomains increases with volume fraction of polymer in the gel. It is suggested that more experiments need to be conducted to investigate the effect of the gel composition and the release

behavior of different solutes.

6.4 MATHEMATICAL MODEL

The purpose of this model is to introduce a theoretical approach in order to predict the drug release from our hydrogels. More specifically we want to investigate if there is a gel configuration that will allow release of solute from the microdomains to the bulk phase, at a rate fast enough to keep the bulk concentration always saturated as the solute diffuses to the surroundings. The parameters that we can manipulate in our model include the volume fraction of the microdomains, thus the total interfacial area between the microdomains and the bulk as well as the interfacial area between the gel and the surroundings. Moreover the release will depend on the hydrophobicity of the solvent, thus the partition coefficient at the interface between the bulk and the microdomains may also be manipulated. The overall gel dimensions and its geometry have been shown to play an important role in the release as well (81). In the present study a cylindrical device of radius R, with spherical microdomains dispersed throughout (Figure 5) has been examined for controlling solute release.

The solute is loaded into the gel and the concentration of the solute in the microdomains is assumed to be higher than its saturation concentration in water. We consider that the drug

diffuses from the microdomains into the bulk phase and then to the surface of the cylinder. The diffusing drug is instantaneously removed once it reaches the surface of the cylinder. If we assume that diffusion through the bulk is much slower than diffusion into the bulk phase, we can neglect the latter, and then the non-steady, one-dimensional problem is described by Fick's Law of diffusion. We also introduce another equation to account for the depletion of the drug from the microdomains, that relates the concentration of the microdomains and that of the bulk phase. Thus the governing equations of the system are the following:

$$(1-\phi)\frac{\partial c_b}{\partial t} = D_b \nabla^2 c_b + h(c_b - \alpha c_m) \tag{6.1}$$

$$\phi \frac{\partial c_m}{\partial t} = -h(c_b - \alpha c_m) \tag{6.2}$$

where the above variables and parameters are defined as:

c_b = the concentration of the solute in the bulk phase, g/cm^3

c_m = the concentration of the solute in the microdomains, g/cm^3

ϕ = volume fraction of the microdomains

D_b = the diffusivity of the solute in the bulk phase, cm^2/sec

h = the mass transfer coefficient at the microdomain/bulk interface in the gel, cm/sec

α = the overall partition coefficient of the solute between the two phases in the gel.

r = radial distance from the center of the device, cm

t = time, sec

Equations 6.1 and 6.2 are subject to the following boundary and initial conditions:

$$c_b(r=R, t) = 0 \tag{6.3}$$

$$c_b(r, t=0) = c^* \tag{6.4}$$

$$c_m(r, t=0) = \frac{c^*}{\alpha} \tag{6.5}$$

$$r=0;\ \frac{dc_b}{dr} = 0 \tag{6.6}$$

where c^* is the saturation concentration in water. The first condition states that the surface concentration (r=R) is zero, because in practice the drug will be convected away by the flowing blood. The second states that the initially the concentration of the solute in the hydrophilic phase is equal to its saturation concentration in water. The third condition describes the interfacial partitioning from the hydrophobic phase to the hydrophilic one, (α<1), and the last condition arises from the fact that the flux has to be zero at the center of the cylinder.

By introducing the dimensionless variables $\tilde{c}_b=c_b/c^*$, $\tilde{r}=r/R$, $\tilde{c}_m=c_m/c^*$, $\tau=D_bt/R^2$, $\lambda= hR^2/D_b$, where $\tilde{c}_b$ and $\tilde{c}_m$ are the dimensionless concentrations, $\tilde{r}$ is the dimensionless radial distance, τ is the dimensionless time, and λ is a dimensionless number, equations 6.1-6.6 become:

$$(1-\phi)\frac{\partial \tilde{c}_b}{\partial \tau} = \frac{\partial^2 \tilde{c}_b}{\partial \tilde{r}^2} + \frac{1}{\tilde{r}}\frac{\partial \tilde{c}_b}{\partial \tilde{r}} + \lambda(\tilde{c}_b - \alpha \tilde{c}_m) \tag{6.7}$$

$$\phi \frac{\partial \tilde{c}_m}{\partial \tau} = -\lambda(\tilde{c}_b - \alpha \tilde{c}_m) \tag{6.8}$$

with initial and boundary conditions:

$$\tilde{c}_b(\tilde{r}=1, \tau) = o \tag{6.9}$$

$$\tilde{c}_b(\tilde{r}, \tau=0) = 1 \tag{6.10}$$

$$\tilde{c}_m(\tilde{r}, \tau=0) = \frac{1}{\alpha} \tag{6.11}$$

$$\tilde{r}=0; \frac{\partial \tilde{c}_b}{\partial \tilde{r}} = 0 \tag{6.12}$$

6.5 Solution of the Problem

Equations 6.7 and 6.8 have been solved simultaneously by means of Laplace transforms (84-86). The equations in the Laplace domain with the use of the initial conditions are:

$$(1-\phi)(s\bar{c}_b - 1) = \frac{d^2\bar{c}_b}{d\tilde{r}^2} + \frac{1}{\tilde{r}}\frac{d\bar{c}_b}{d\tilde{r}} + \lambda(\bar{c}_b - \alpha \bar{c}_m) \tag{6.13}$$

$$\phi(s\bar{c}_m - \frac{1}{\alpha}) = -\lambda(\bar{c}_b - \alpha \bar{c}_m) \tag{6.14}$$

where the (˜) above c_b and c_m has been dropped for simplicity, in favor of the (-) and the (s) which denote Laplace domain. By

eliminating c_m from the above equations we obtain:

$$\bar{c}_b'' + \frac{1}{\tilde{r}}\bar{c}_b' - M^2\bar{c}_b = \frac{\lambda\phi}{\phi s+\lambda\alpha} - (1-\phi) \tag{6.15}$$

where the (") and (') denote second and first derivatives with respect to r, and M is defined as follows:

$$M=\left(s(1-\phi) -\lambda+\frac{\lambda^2\alpha}{\phi s+\lambda\alpha}\right)^{1/2} \tag{6.16}$$

The homogeneous part of equation 6.15 is the well known modified Bessel function of order zero. The complete solution of this equation in the Laplace domain after applying the boundary conditions is:

$$\bar{c}_b = \frac{1}{s}\left(1-\frac{I_0(M\tilde{r})}{I_0(M)}\right) \tag{6.17}$$

This equation needs to be inverted in to the time domain to obtain $\tilde{c}_b(\tilde{r},\tau)$. Then the solution of equation 6.8 is:

$$\tilde{c}_m = \frac{1}{\alpha}e^{-\frac{\lambda\alpha}{\phi}\tau} + \frac{\lambda}{\phi}\int_0^\tau \tilde{c}_b e^{-\frac{\lambda\alpha}{\phi}(\tau-\tau')}d\tau' \tag{6.18}$$

Inversion of equation 6.17 is done using the theorem of inverse Laplace transforms. A detailed description of the inversion is given in appendix B. The concentration c_b is given by:

$$\tilde{c}_b(\tilde{r},\tau) = -\sum_{n=1}^{\infty}\frac{e^{s_1^n\tau}I_0(M\tilde{r})}{s_1^n M I_0'(M)} - \sum_{n=1}^{\infty}\frac{e^{s_2^n\tau}I_0(M\tilde{r})}{s_2^n M I_0'(M)} \tag{6.19}$$

where s_1 and s_2 are the roots of the equation, $M(s)=-i\xi_n$, (ξ_n are the positive roots of I_0), and are functions of α, ϕ, λ, h and D_b

(Appendix B).

The mathematical model developed here describes the concentration profile of a solute released from a cylindrical device. The concentration profile depends on the partition coefficient of the solute between the two phases in the gel, α, the volume fraction of the microdomains, ϕ, and the dimensionless parameter λ ($= hR^2/D_b$). All these parameters may be manipulated by the solute structure and the gel composition. The partition coefficient can be evaluated from solute uptake measurements. The mass transfer coefficient, h, depends on the structure of the domain/bulk interface and will change if we use a different polymer, such as one with different structure side chain. The volume fraction of the microdomains, ϕ, can be estimated from the weight fraction of the microdomains (as measured by rheology) and an estimated density of the domains from known hydrocarbon or surfactant densities. Thus the release rate may be easily controlled by an optimum selection of these design parameters. The next task is to determine numerically over what values of the above parameters the flux ($N_b = \partial\tilde{c}_b/\partial\tilde{r}$) is constant over time.

Table 6.1

Solute-loading results

Solute (gel)	Gel Volume (ml)	Conc. in soak solution (g/L)	Conc. in the gel (g/L)	Conc. ratio: gel/ sat. water
Trypt. (1)	15	10.1	18.8	1.6
(2)	16	9.8	19.8	1.7
(3)	19	9.5	19.5	1.7
Theoph.(1)	20	6.0	11	1.6
(2)	21	6.2	10	1.4
(3)	19	6.3	10.6	1.5

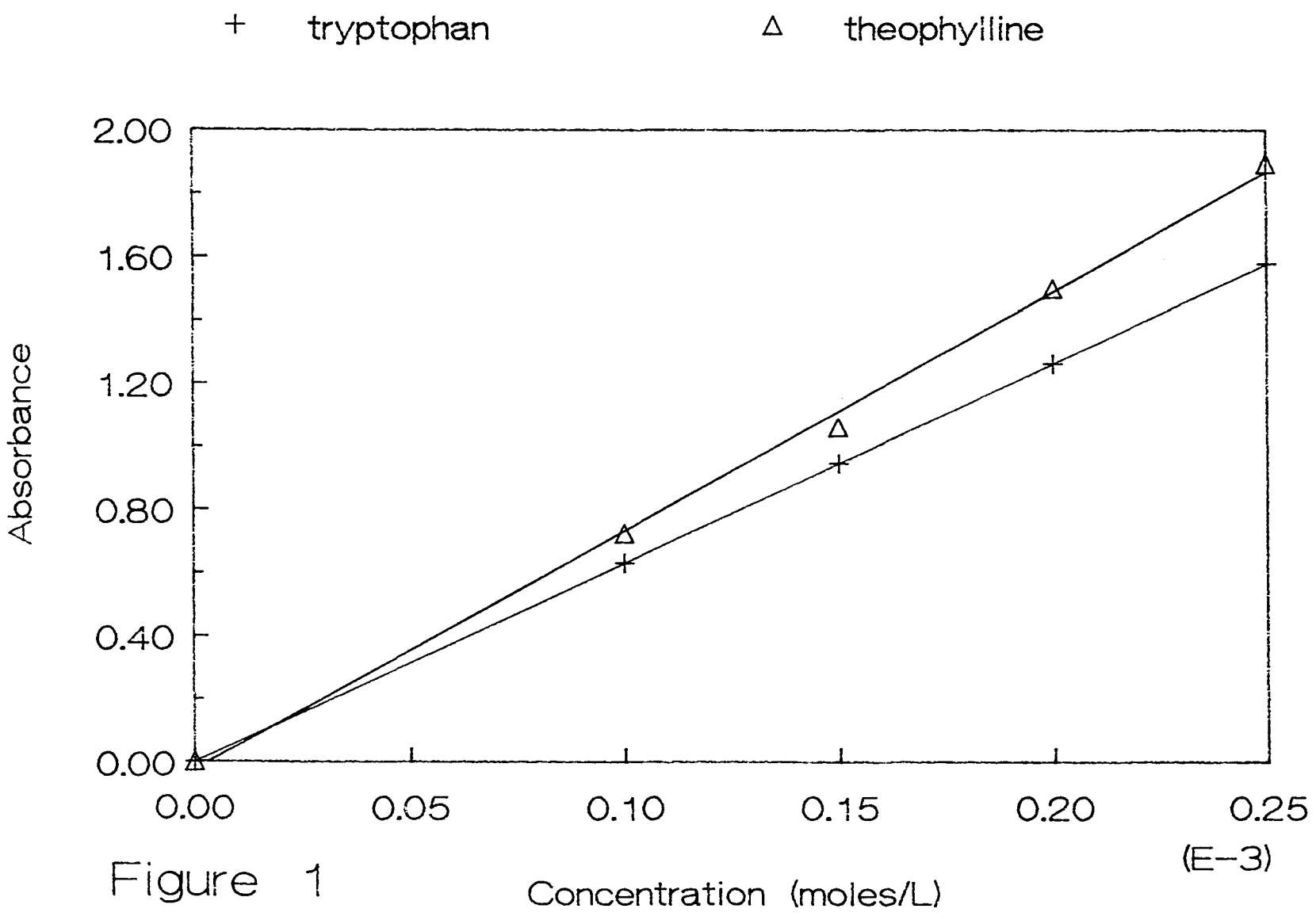
+ tryptophan
Δ theophylline
2.00
1.60
1.20
0.80
0.40
0.00
Absorbance
0.00
0.05
0.10
0.15
0.20
0.25
(E-3)
Concentration (moles/L)

Figure 1

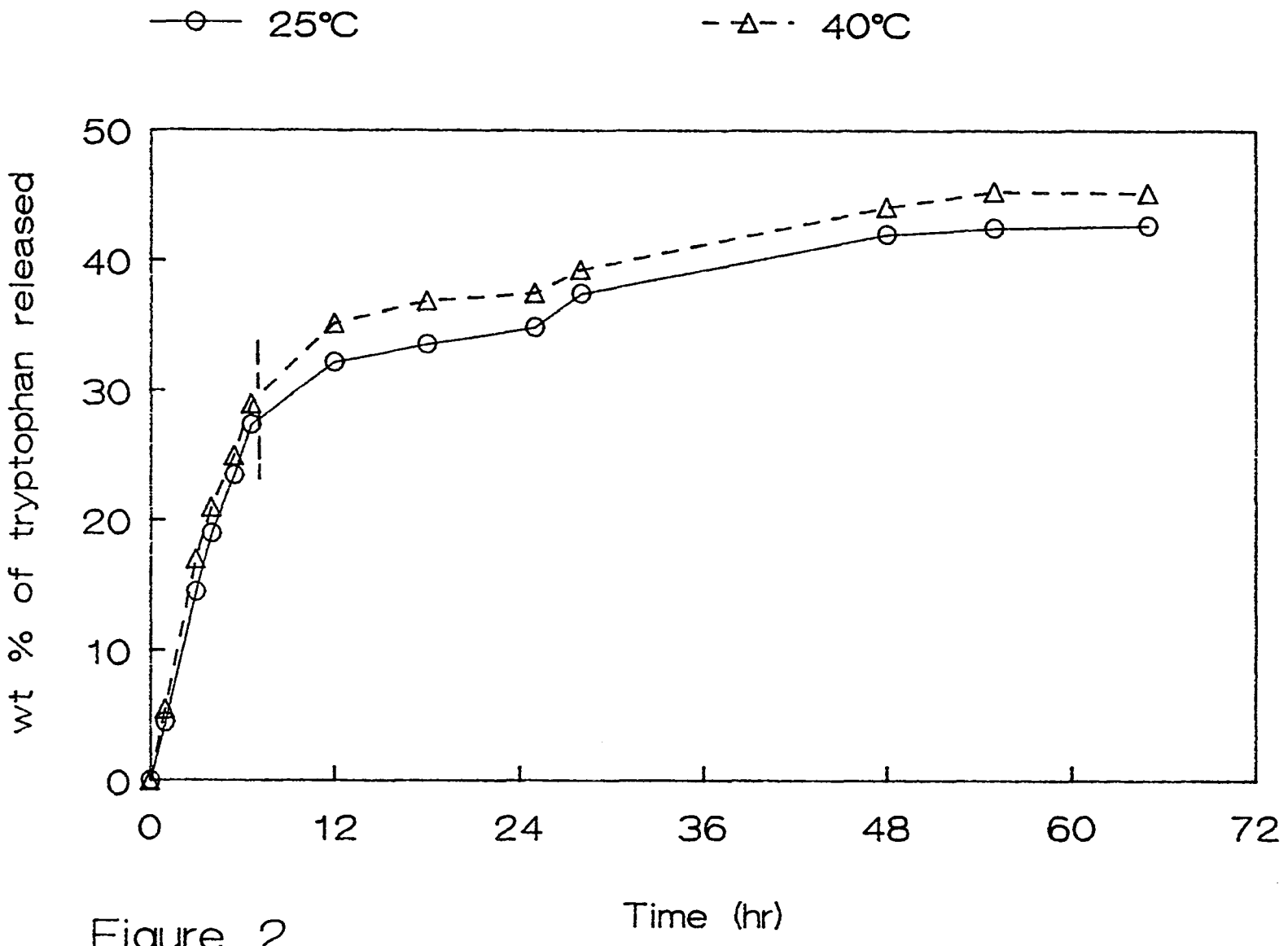
25°C
40°C
wt % of tryptophan released
50
40
30
20
10
0
0
12
24
36
48
60
72
Time (hr)

Figure 2

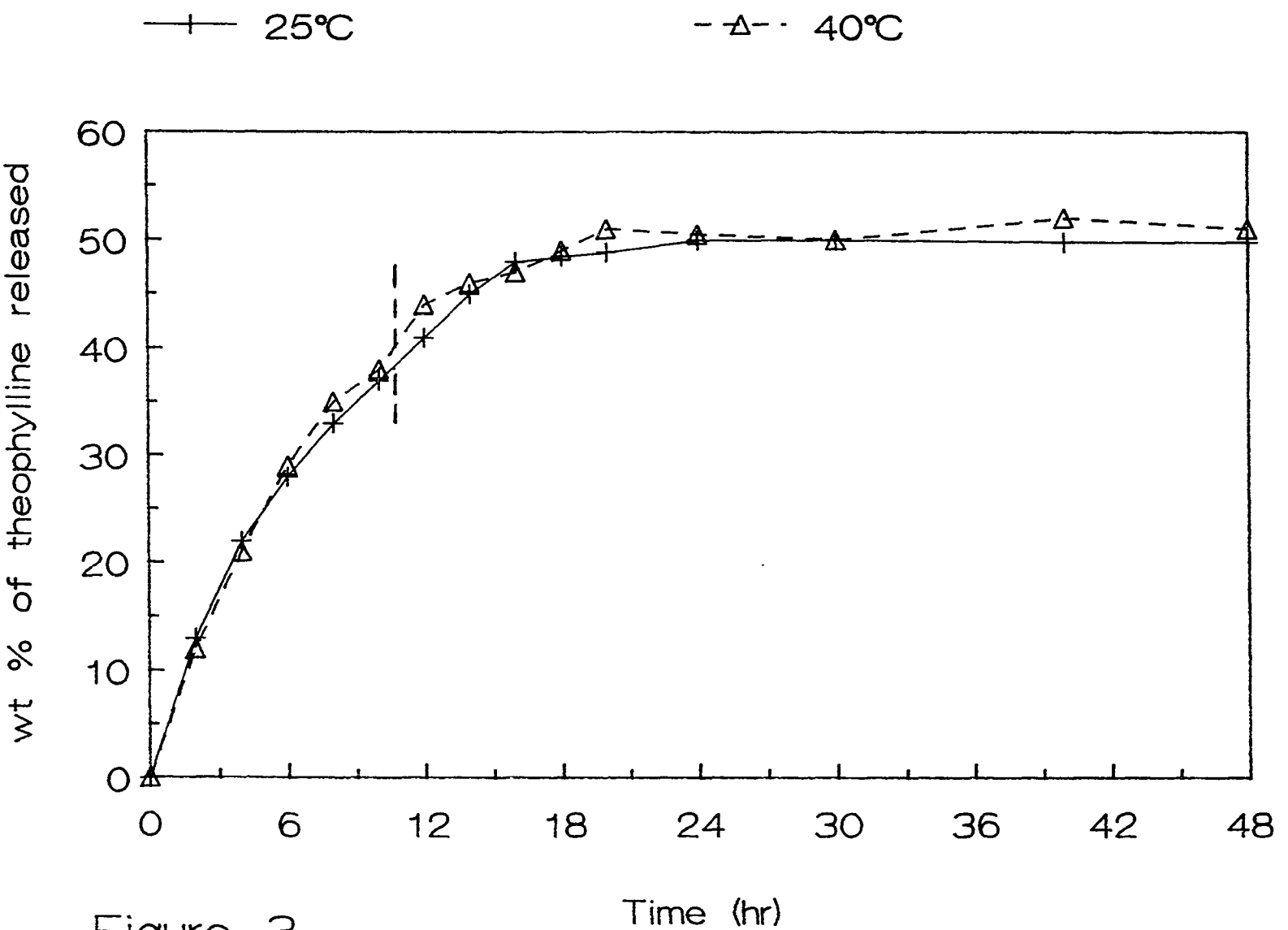
25℃
40℃
wt % of theophylline released
60
50
40
30
20
10
0
0
6
12
18
24
30
36
42
48
Time (hr)

Figure 3

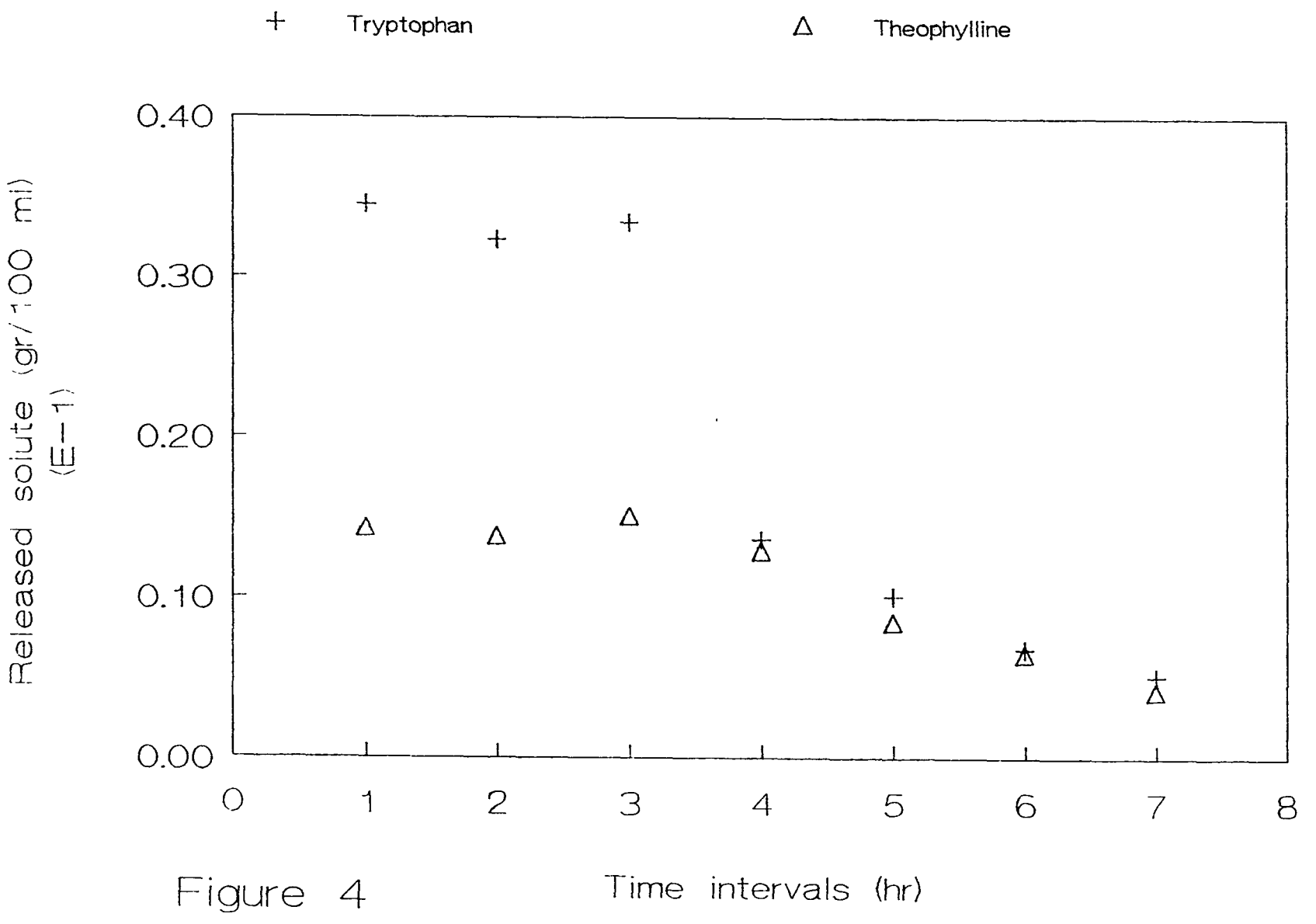
+ Tryptophan
Δ Theophylline
Released solute (gr/100 ml) (E-1)
0.40
0.30
0.20
0.10
0.00
0
1
2
3
4
5
6
7
8
Time intervals (hr)

Figure 4

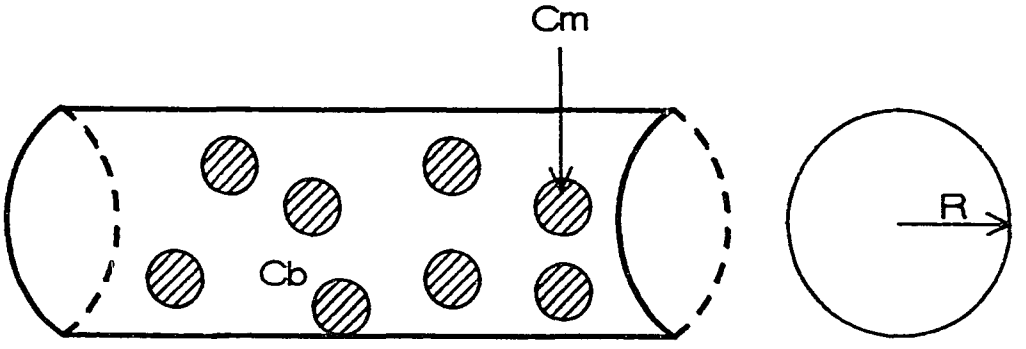

Figure 5

Chapter 7

SUMMARY CONCLUSIONS AND RECOMMENDATIONS FOR FUTURE WORK

Biphasic hydrogels have been prepared from a hydrocarbon-grafted water soluble cellulose ether in ethanol/water solvents. The bulk and microscopic properties of the materials have been investigated using rheological and fluorescence probe techniques. Results presented in chapters 4-6 have shown that the hydrogels behave like viscoelastic materials, are composed of hydrophobic microdomains dispersed throughout a hydrophilic polymer network and have the ability to absorb and release permeants. This property makes these materials of value in controlled release and chromatographic separation processes. Further investigation of their properties and applications is recommended and is discussed below.

In order to draw a complete structural picture of our hydrogels the size (radius of gyration) and the geometry of the aggregates need to be determined. The radius of gyration and the hydrophobicity of the domains will determine in part the structure of solutes which may be incorporated. For example, the microdomains will not be able to incorporate drugs with greater molecular weight than their own. Evaluation of these parameters may be accomplished by conducting small angle neutron scattering experiments. A detailed description of these experiments is

presented in appendix A.

The preliminary release experiments have shown that constant solute release is accomplished for short times only. Additional release experiments are recommended, using solutes with different degree of hydrophobicity to investigate if constant release can be obtained over prolonged times. In addition, the effect of the gel composition as discussed in chapter 6 needs to be investigated. Also from the mathematical model we see that the release rate is a function of the hydrophobicity of the solute and the number of the microdomains present in the system. Thus, the model needs to be compared to experimental results obtained using polymer networks with different number of microdomains and solutes with different degree of hydrophobicity. This will determine the regions over which the released flux is constant over time.

As discussed in chapter 4, dialysis experiments may be used to clarify the surface tension results. Our results in chapter 4 were interpreted based on the theory developed by Roberts, G.A.F. and Thomas, I.M.. According to that theory the polymer is maximally solubilized in a solvent when the absolute value of the change in surface tension of the polymer solution and the pure solvent ($\gamma-\gamma_0$) shows a minimum. In our system (ethanol-water-polymer) the unusual surface activity of the solutions which shows a rise in surface tension as the polymer concentration

increases could be attributed to a sequestering of the ethanol in hydrophobic clusters within the network. This hypothesis may be tested with the dialysis experiments discussed in chapter 4.

APPENDIX

A. Small Angle Neutron Scattering

The high penetration into materials by the neutron is the key property in many applications of small angle neutron scattering (SANS). It enables scattering from a volume of material within the sample to be investigated. This volume may be small, so that the variation with position of some property, such as strain, of the sample may be determined. The strength of the interaction between a neutron and a single nucleus is specified by the empirically determined scattering length b, which is called coherent scattering length and has been determined for many atomic nuclei. The scattering length is different not only for each atom but also for each isotope. Therefore by changing the isotopic composition we have the possibility of varying the scattering length of the matrix or solvent without changing the basic properties of the system. This technique can be used to great effect when studying copolymers in solutions. The method which is called contrast matching will be described in detail below. Besides the coherent scattering that arises from the so-called average nucleus, there is also incoherent scattering present. Incoherent scattering contains two components: a contribution due to a random distribution of the deviations of the scattering lengths from their mean value, and the other arising from the fluctuations of

the nuclear spins.

Small angle neutron scattering (SANS) experiments may be used to measure the molecular weight and the geometry of the hydrophobic aggregates dispersed within the polymer gel. The molecular weight will be determined using the contrast matching technique. The geometry of the aggregates will be deduced from the scattering intensity distribution. A brief description of the general analysis of SANS experiments and these methods is given below.

The object of small-angle scattering experiments is to obtain the scattering due to a particle alone when it is in the presence of a solvent. The excess scattering of the solution over that of the solvent is the particle scattering. The amplitude of the neutron waves that are scattered by a nucleus is characterized by the sum of scattering lengths, b_{total}. This sum gives the density of the scattering length, ρ, from:

$$\rho = \frac{b_{total}}{v} \qquad (A.1)$$

where v is the molecular volume and b_{total} is the sum of two components defined previously: $b_{coherent}$ and $b_{incoherent}$. The first contains structural information (the relative arrangement of the nuclei with respect to each other, which leads to the geometry, molecular weight, etc), while the second gives rise to a background which is independent of the scattering angle. Because only the coherent scattering is used to derive structure properties, it is necessary to subtract the incoherent

scattering. Generally, the incoherent scattering is considered to arise entirely from the solvent, so that a measurement with a sample containing only the solvent allows its determination.

In the contrast matching method experiments are based on the important difference between the coherent scattering length of different isotopes. Thus, for example, for aqueous systems, mixtures of H_2O and D_2O will provide different average scattering lengths depending on their composition without modifying significantly the thermodynamic properties. The coherent intensity, $I_{coherent}$, is proportional to the square of the difference between the coherent scattering length density of the polymer, ρ and the coherent scattering length density of the solvent, ρ_s (31,32).

$$I_{coherent} = (\rho - \rho_s)^2 \qquad (A.2)$$

This relationship is very significant because in a system with n different solutes we can find a set of solvents whose scattering length density can match n-1 solutes. In this solvent the n-1 components of the system will not produce any coherent scattering at small angles and all the observed coherent scattering will be produced by the one component whose scattering density does not match that of the solvent. Then information about the structure of that specific component can be derived. In our system we will be able to derive information for both the hydrophobic (aggregates) and the hydrophilic (backbone) part of the polymeric gels. This will be accomplished first, by finding an appropriate mixture of H_2O-D_2O whose scattering density matches that of the

hydrophilic part of our polymer. That will enable us to measure the intensity I(Q) as a function of the scattering vector (Q) of the hydrophobic aggregates. Here Q is the Bragg wave vector given by:

$$Q = \frac{4\pi \sin(\theta/2)}{\lambda} \qquad (A.3)$$

where λ is the wavelength and θ is the scattering angle. The available wavelength range of neutrons is between 5 and 15 A (30). This provides scattering vectors Q of the order $2x10^{-3}$ to $5x10^{-1}$ A-1 which are suitable for the characterization of aggregates. Extrapolation of the data to zero Q (i.e. zero scattering angle) will give us I(0) which is the coherent intensity scattered at zero angle. The molecular weight, M, of the aggregates is related to I(0) by the following equation:

$$\frac{I(0)}{C} = AM(\rho - \rho_s)^2 \qquad (A.4)$$

where c is the polymer concentration and experimental factor for the incoherent scattering given by:

$$A = \frac{4\pi T_s N_A t}{1-T} \qquad (A.5)$$

where T_s and T are the measured transmissions of the sample and the solvent, respectively, t is the thickness of the sample, and N_A is Avogadro's number. The method described above was developed by Jacrot and Zaccai (32).

The geometry of the aggregates can also be deduced from the scattering intensity distribution over a range of scattering

angles. This is done by choosing a theoretical structural model and fitting the experimental data. This analysis has been done for particles with various geometries such as cylindrical, spherical, and ellipsoidal (34-37). I(Q) can be written:

$$I(Q) = I(0)\, P(Q)\, S(Q) \qquad (A.6)$$

where S(Q) is an interparticle structure factor of the scattering particles, and P(Q) is a so called geometrical form factor (spherical, cylindrical, etc). In dilute solutions, due to the weak interparticle interactions, the factor S(Q) is assumed to be unity. Also it has been shown experimentally (37) that even in concentrated solutions as Q increases $S(Q) \rightarrow 1$. Thus the factor is unity for all Q in the dilute solutions and at sufficiently large Q in the case of high concentrations. Expressions for the form factors of different geometries are given in the literature. Also molecular parameters needed for our calculations are given in table A1.

Small angle neutron scattering experiments (SANS) may me carried out at the Brookhaven National Laboratory (BNL). Using SANS experiments we can determine the molecular weight and the shape of our aggregates. With this information we will be able to draw a more complete structural picture of our systems.

TABLE 3

Neutron Scattering Parameters

SPECIES	MOLECULAR VOLUME (nm^3)	$b_{coherent}$ (fm)	SCATTERING LENGTH DENSITY
CH_3	0.0543	-4.574	-84
CH_2	0.0269	-0.8334	-31
H_2O	0.0299	-1.677	-56
D_2O	0.0302	19.153	634
CRU*	1.725	49.71	28.8

* CRU: Cellulose Repeat Unit (2 anhydroglucose units)

B. Method of inversion from the Laplace to the time domain

The equation needed to be inverted is 6.17. That is:

$$\overline{c}_b = \frac{1}{s}\left(1 - \frac{I_0(M\tilde{r})}{I_0(M)}\right) \tag{6.17}$$

where M is a function of s, defined by equation 6.16. Using reference (85) we proceeded as follows. First we need to find the poles of the function by setting: $M(s) = i\xi_n$, where ξ_1, ξ_2,... are the positive zeros of I_0. Thus, we need to solve the following equation:

$$\left(s(1-\phi) + \frac{\lambda^2\alpha}{\phi s+\lambda\alpha} - \lambda\right)^{\frac{1}{2}} = i\xi_n \tag{B.1}$$

Squaring both sides of this equation and solving the resulting quadratic equation for $s_{1,2}$ we have:

$$s_{1,2} = \frac{(\phi\xi_n^2 - \delta) \pm \sqrt{(\delta - \phi\xi_n^2)^2 - 4\beta\alpha\lambda\xi_n^2}}{4\beta} \tag{B.2}$$

where $\beta = \phi(1-\phi)$ and $\delta = \lambda(\alpha - \alpha\phi - \phi)$. Thus, the poles are at 0, and $s_{1,2}$. The inverse Laplace is given by:

$$\mathcal{L}^{-1}\left(\frac{I_0(M\tilde{r})}{sI_0(M)}\right) = \left(Res_0 + \sum_{n=1}^{\infty} Res_{s_1^n} + \sum_{n=1}^{\infty} Res_{s_2^n}\right)\left(\frac{I_0(M\tilde{r})\, e^{s\tau}}{sI_0(M)}\right) \tag{B.3}$$

The next step involves evaluation of the residue at the poles. To find the residue at zero we multiply the expression by s and then we take the limit as $s \to 0$. Then $Res_0 = 1$. Same way for the residue at s_1^n and s_2^n after expanding $I_0(M(s))$ using Taylor's

series and take the limit as the poles approach zero, we obtain:

$$
\begin{aligned}
& Res_{s_1^n}\left(\frac{I_0(M\tilde{r})}{sI_0(M)}e^{s\tau}\right) \\
&= e^{s_1^n\tau}\lim_{s\to s_1^n}\left(\frac{(s-s_1^n)\,I_0(M\tilde{r})}{sI_0[M(s)]}\right) \qquad \text{(B.4)} \\
&= e^{s_1^n\tau}\frac{I_0[M(S_1^n)\,\tilde{r}]}{s_1^n\,M'(s_1^n)\,I_0'[M(s_1^n)]}
\end{aligned}
$$

Similarly the same equation is obtained for the residue at s_2^n. By substitution of the residue values in equation (B.3), coupled with the fact that the inverse Laplace transform of 1/s is one, we obtained equation (6.19) which is the solution of the problem.

BIBLIOGRAPHY

1. Shibanov, Y.D. and Godovsky, Y.K. Colloid Polym. Sci. 263 202 (1985)
2. Henderson, C.P. and Williams, M.C. Polymer 26 2021 (1985)
3. Henderson, C.P. and Williams, M.C. Polymer 26 2026 (1985)
4. de la Cruz, M. and Sanchez, I.C. Macromolecules 19 2501 (1986)

4a. Krause,S. in Colloidal and Morphological Behavior of Block and gragt Copolymers Molau, G.E., eds. Plenum Press (New York-London) p.223 (1971)

5. M. Jiang et al. Polymer 26 1689 (1985)
6. Sariban, A. and Binder, K. Macromolecules 21 711 (1988)
7. Tuzar, Z., Stepanek, P., Konak, C., and Kratochvil, P. J. Colloid Interface Sci. 105 372 (1985)
8. Sanchez, I.C. Macromolecules 17 967 (1984)
9. Roche, E.J., Pineri, M. and Duplessix, R. J. Polym. Sci.: Polym. Phys. Ed. 20 107 (1982)
10. Hopfenberg, H.B. and Paul, D.R. in Polymer Blends, vol. 1 Paul, D.R. and Newman, S., eds. Academic Press (New York) p. 445 (1978)
11. Steiner, C.A. Polymer Preprints 26:1 224 (1985)
12. Eliassaf, J. Polymer Letters 3:767 (1965)
13. Ikemi, M., Odagiri, N., Tanaka, S., Shinohara, I., Chiba, A. Macromolecules 14 34 (1981)

14. Ikemi, M., Odagiri, N., Tanaka, S., Shinohara, I. Polymer J. 12 777 (1980)

15. Ikemi, M., Odagiri, N., Tanaka, S., Shinohara, I., Chiba, A. Macromolecules 15 281 (1982)

16. Noolandi, J. and Hong, K.M. Macromolecules 16 1443 (1983)

17. Plestil, J., Baldrian, J. Makromol. Chem. 176 1009 (1975)

18. Leibler, L. Macromolecules 13 1602 (1980)

19. Misra, B.N., Mehta, I.K. and Khetarpal, R.C. J. Polym. Sci: Polym. Chem. Ed. 22 2767 (1984)

20. Krause, S.J. and Haddock, T. J. Polym. Sci B: Polym. Phys. 24 1991 (1986)

21. Dualeh, A.J. and Steiner, C.A. Macromolecules 23 251 (1990)

22. Steiner, C.A. and Gelman, R.A. Cellulosics Utilization: Research and Rewards in Cellulosics; Inagaki, H., Philips, G.O., Eds.; Elsevier: London, 1989; p. 132

23. Lakowicz, J.R. Principles of Fluorescence Spectroscopy Plenum Press, New York, p. 1

24. Kalyanasundaram, K. and Thomas, J.K. J. Am. Chem. Soc. 99 2039 (1977)

25. Binana-Limbele, W. and Zana, R. Macromolecules 20 1331 (1987)

26. Chiu, G., Winnik, M.A. and Croucher, M.D. Colloid and Polym. Sci. 264:25 (1986)

27. Abuin, E., Lissi, E., Blanchi, N., Miola, L. and Quina, H. J. Phys. Chem. 87 5166 (1983)

28. Thomas, J.K. Chem. Rev. 80 283 (1980)

29. Chen, T. and Thomas, J.K. J. Polym. Sci.: Polym. Chem. Ed. 17 1103 (1979)

30. Ionescu, L., Picot, C., Duval, M., Duplessix, R., Benoit, H. and Cotton, J. P. J Polym. Sci.: Polym. Phys. Ed. 19 1019 (1981)

31. Cabane, B. and Duplessix, R. J. Physique 43 1529 (1982)

32. Jacrot, B. and Zaccai, G. Biopolymers 20 2413 (1981)

33. Saito, S. J. Colloid Interface Sci. 24 227 (1967)

34. Shih, L.B., Mauer, D.H., Verbrugge, C.J., Wu, C.F., Chang, S.L. and Chen, S.H. Macromolecules 21 3235 (1988)

35. Shih, L.B., Sheu, E.Y. and Chen, S.H. Macromolecules 21 1387 (1988)

36. Higgins, J.S., Dawkins, J.V., Maghami, G.G. and Shakir S.A. Polymer 27 931 (1986)

37. Brown, J.C., Pusey, P.N., Godwin, J.W. and Ottewill, R.H. J. Phys. A. 8 664 (1975)

38. Lantman, C.W. et al. Macromolecules 21 1339 (1988)

39. Higgins, J.S. and Maconnachie, A. Polymer in Solutions Forsman, W.C. ed. Plenum Press, New York, (1986) p. 183

40. Graessley, W.W. and Rovers, J. Amer. Chem. Soc. 12 959 (1979)

41. Ferry, J.D. Viscoelastic Properties of Polymers John Willey, (1970)

42. Rodriguez, F. Principles of Polymer Systems, McGraw-Hill, New York, p. 201 (1982)

43. Rouse, P.E. J. Chem. Phys. 21 272 (1952)

44. Graessley, W.W. Polymers in Solutions Forsman, W.C. ed. Plenum Press, New York, p. 145 (1986)

45. Westman, L. and Lindstrom, T. J. Appl. Polym. Sci. 26 2519 (1981)

46. Dayan, S., Gilli, J.M. and Sixou, P. J Appl. Polym. Sci. 28 1527 (1983)

47. Aharoni, S.M. Polymer 21 1413 (1980)

48. Graessley, W.W. Macromolecules 15 1164 (1982)

49. Graessley, W.W. and Roovers, J. Macromolecules 12 959 (1979)

50. Buckles, R.G. J. Biomed. Materials Research 17 109 (1983)

51. Graham, N.B. and McNeil, M.E. Biomaterials 5, 27-36 (1984).

52. Korsmeyer, R.W. and Peppas, N.A. J. Controlled Release 1, 89-98 (1984).

53. Lee, P.I. J. Controlled Release 2, 277-288 (1985).

54. Folkman, J. and Long, D.M. J. Surg. Res. 4, 139-142 (1964).

55. Ermini, M. and Carpino, F. Acta Endorcinol. 13, (2), 360-373 (1973).

56. Croxato, H. and Diaz, S. Am. J. Obstet. Gynecol. 106, 1135 (1969).

57. Langer, R.S. Chem. Eng. Commun. 6:1 (1980).

58. Langer, R.S. and Peppas, N.A. Biomaterials 2:201 (1981).

59. Langer, R.S and Peppas, N.A. J. Macromol. Sci., Rev. Macromol. Chem. 16:00 (1983).

60. Peppas, N.A. and Gurny, R. Pharm. Acta Helv. 58:2 (1983).

61. Korsmeyer, R.W. and Peppas, N.A. in Controlled Release

Systems, Mansdorf, S.Z. and Roseman, T.J. eds., Dekker, M. New York, NY, p.77 (1983).

62. Gurny, R., Doelker, E. and Peppas, N.A. Biomaterials 3:27 (1982).

63. Peppas, N.A. Controlled Drug Bioavailability 1:000 (1983).

64. Franson, N.M. and Peppas, N.A. J. Appl. Polym. Sci. 28:000 (1983).

65. Peppas, N.A. Recent Adv. Drug Delivery Systems, Proc. Int. Symp. p. 279 (1984).

66. Chen, D. and Kennedy, P. J. Biomedical Mat. Research, Vol. 23, 1327-1342 (1989).

67. Ueno, N., Refojo, M. and Liu, H.S. J. Biomed. Mat. Research, Vol. 16, 669-677 (1982).

68. Baker, R.W. and Lonsdale, H.K. Controlled Release of Biolog. Act. Agents, Tanquary, A.C. and Lacey, R.E., Plenum, N.Y., 1974, pp. 15-71.

69. Chien, Y.W. Drug Delivery Systems, Juliano, R.L., Ed. Oxford U.P., New York, 1980, pp. 11-83.

70. M.E. de Vries and H.E. Bodde J. Biomed. Mat. Research, Vol. 22, 1023-1032 (1988).

71. Park, G.B. Biomat. Mad. Dev. Art. Org., 6, 1 (1978).

72. Behar, D., Juszynski, M., Ben Hur, N., Golan, J., and Rudenski, B. J. Biomed. Mat. Research, Vol. 20, 731-738 (1986).

73. Ruckenstein, E. and Gourisankar, S.V. J. Colloid Interphase Sci. 109:557 (1986)

74. Okano, T., Nishiyama, S., Shinohara, I., Akaike, T., and Sakurai, T. Polymer J. 10:223 (1978)

75. Yokoyama, M. , Nakahashi, T., Nishimura, T., Maeda, M. and Inoue, S. J. Biomed. Mater. Res. 20:867 (1986)

76. Gregonis, D.E., Coleman, D.L., Hsu, R. and Buerger, D., Hydrophobic Hydrogels: Physical Characteristics and Blood Interaction, Appl. Polym. Sci. Proc. Org. Coatings, (ACS) 1983 48 643-6

77. Roberts, G.A.F. and Thomas, I.M. (1978) Polymer 19 459

78. Varelas, C.G. and Steiner, C.A. in Absorbent Polymer Technology, L. Brannon-Peppas and R.S. Harland, eds., Elsevier (Amsterdam) 1990 p. 259

79. Varelas, C.G. and Steiner, C.A. J. of Polym. Science B: Polym. Physics, in review.

80. Varelas, C.G., Dualeh, A.J. and Steiner, C.A., Polym. Prepr. 31 (Am. Chem. Soc., Div. Polym. Chem.) 1991 (1981).

81. Tojo, K. Chem. Eng. Commum. Vol. 30, p. 311 (1984)

82. Lee, P.I. J. Controlled Release 2, 277-288 (1985).

83. Dong, L.C. and Hoffman, A.S. J. of Controlled Release, 13 21-31 (1990)

84. Crank, J., Mathematics of Diffusion, 2nd edn., Clarendon Press, Oxford (1975)

85. Sneddon, I.N., The Use of Integral Transforms, TMH edition.

86. Carslaw, H.S. and Jaeger, J.C., Conduction of Heat in

Solids, Clarendon Press, Oxford (1959).

87. Peppas, A.N. and Franson, M.N., J. of Polymer Science: Polymer Phys. Edn. 21 (1983)

88. Shah, S.S., Kulkarni, M.G. and Mashelkar, R.A., J. of Controlled Release, 12 (1990)